AD-A214 692

REPORT DOCUMENTATION PAGE

Form Approved
OMB No. 0704-0188

1. AGENCY USE ONLY (Leave blank)	2. REPORT DATE	3. REPORT TYPE AND DATES COVERED
	29 May 1981	Final (1 Oct 79- 30 Sep 80)

4. TITLE AND SUBTITLE

BACKGROUND SKY BRIGHTNESS MEASUREMENTS FOR APPLICATION TO SPACE SURBEILLANCE SYSTEMS

5. FUNDING NUMBERS

61102F
2311/A1

6. AUTHOR(S)

J.L. Weinberg
D.W. Schuerman

7. PERFORMING ORGANIZATION NAME(S) AND ADDRESS(ES)

Space Astronomy Laboratory
State University of New York at Albany
Albany, NY 12203

8. PERFORMING ORGANIZATION REPORT NUMBER

9. SPONSORING/MONITORING AGENCY NAME(S) AND ADDRESS(ES)

AFOSR
BLDG 410
BAFB DC 20332-6448

10. SPONSORING/MONITORING AGENCY REPORT NUMBER

afosr 80-0043

11. SUPPLEMENTARY NOTES

12a. DISTRIBUTION/AVAILABILITY STATEMENT

12b. DISTRIBUTION CODE

13. ABSTRACT (Maximum 200 words)

DISTRIBUTION STATEMENT A
Approved for public release;
Distribution Unlimited

14. SUBJECT TERMS	15. NUMBER OF PAGES
	58
	16. PRICE CODE

17. SECURITY CLASSIFICATION OF REPORT	18. SECURITY CLASSIFICATION OF THIS PAGE	19. SECURITY CLASSIFICATION OF ABSTRACT	20. LIMITATION OF ABSTRACT
unclassified	unclassified		

FINAL SCIENTIFIC REPORT

BACKGROUND SKY BRIGHTNESS MEASUREMENTS FOR APPLICATION TO SPACE SURVEILLANCE SYSTEMS

U. S. Air Force Office of Scientific Research
Grant AFOSR 80-0043
to State University of New York at Albany

1 October 1979 - 30 September 1980

J. L. Weinberg
Principal Investigator

D. W. Schuerman
Co-Investigator

Space Astronomy Laboratory
State University of New York at Albany
Executive Park East
Albany, New York 12203

29 May 1981

Final Scientific Report
Grant 80-0043

May 1981

TABLE OF CONTENTS

	Page
SUMMARY	1
OBJECTIVES	1
SIGNIFICANT RESULTS	3

Attachments

Publications Supported Under This Grant:

Weinberg, J. L., Measuring Background Starlight, *Sky and Tel.*, 61, 114, February 1981.

Schuerman, D. W., The Restricted Three-Body Problem Including Radiation Pressure, *Ap. J.*, 238, 337, 1980.

Misconi, N. Y., The Photometric Center of the Gegenschein, *Icarus*, in press, 1981.

Schuerman, D. W., On the Equivalence of Expressions for Inverting the 3-Dimensional Zodiacal Light Brightness Integral, *Planet. Space Sci.*, 28, 1077, 1980.

Weinberg, J. L., and R. C. Hahn, Brightness and Polarization of the Zodiacal Light: Results of Fixed Position Observations from SKYLAB, in *Proc. IAU Symposium No. 90, Solid Particles in the Solar System*, I. Halliday and B. A. McIntosh (eds.), (D. Reidel Publ. Co., Dordrecht), 19, 1980.

Schuerman, D. W., The Effect of Radiation Pressure on the Restricted Three-Body Problem, in *Proc. IAU Symp. No. 90*, 285, 1980.

Schuerman, D. W., Evidence that the Properties of Interplanetary Dust Beyond 1 AU are not Homogeneous, in *Proc. IAU Symp. No. 90*, 71, 1980.

Misconi, N. Y., The Symmetry Plane of the Zodiacal Cloud Near 1 AU, in *Proc. IAU Symp. No. 90*, 49, 1980.

Attachments (cont'd.)

Abstracts of Ph.D. Theses Completed During this Report Period

Toller, G. N., A Study of Galactic Light, Extragalactic Light, and Galactic Structure Using Pioneer 10 Observations of Background Starlight, Ph.D. Thesis (Astronomy), State University of New York at Stony Brook, 1981.

Schaefer, R. W., Calculations of the Light Scattered by Randomly Oriented Ensembles of Spheroids of Size Comparable to the Wavelength, Ph.D. Thesis (Physics), State University of New York at Albany, 1980.

Gustafson, B. Å. S., Scattering by Ensembles of Small Particles: Experiment, Theory, and Application, Ph.D. Thesis (Astronomy), University of Lund, Sweden, 1980.

SUMMARY

The scattering of sunlight by interplanetary dust gives rise to the zodiacal light, a ubiquitous feature of the night sky which is the limiting background for most IR observations. This changing (with wavelength, look direction, and distance from the sun) background can be understood only in the larger context of the physics of interplanetary dust. We have observationally separated the zodiacal light from other astronomical sources, devised a mathematical inversion to extract the maximum amount of information about the dust from space observations, observationally proved that the dust complex is neither homogeneous nor simply distributed through the solar system, and predicted that the dust may tend to accumulate in enormous arcs which span the solar system. The inversion technique is the most promising method to extract from visual and near IR observations the parameters necessary to model the IR emission of interplanetary grains.

OBJECTIVES

The scattering of sunlight by interplanetary dust is referred to as zodiacal light, since the brightness and, therefore, the dust distribution have a maximum near the zodiacal band. *Only* the zodiacal light contains information on the integrated properties of the *whole* ensemble of interplanetary dust. Observations of brightness, polarization, and color contain information about the size, shape, composition, and overall optical properties of the grains. Observations made from different locations in the solar system provide data on the change in zodiacal light with heliocentric distance and, therefore, on the spatial distribution of the dust and on changes in its

optical properties as functions of sun-particle distance and height above or below the ecliptic plane.

We have accumulated a vast library of unique observational data on the brightness, polarization, and color of the zodiacal light, including: extensive ground-based observations of the light of the night sky and of Comet Ikey-Seki (1965 VIII) from Mt. Haleakala, Hawaii, the first multicolor observations of large regions of the sky from space (Skylab), and the first observations of large regions of light with heliocentric distance (Pioneers 10 and 11). Each of these data sets is being used with laboratory and theoretical studies to provide information on the spatial distribution, optical and physical properties, and dynamics of the interplanetary dust.

In October 1976, we began an Air Force-funded program to complete the reduction and analysis of the Pioneer 10/11 and Skylab data and to combine these data with ground-based results and theoretical studies to map zodiacal light brightness and polarization over the sky and to determine the nature and distribution of the interplanetary grains. Studies have been made of the dynamics of small particles in the solar system, and of methods for inverting the zodiacal light brightness integral to derive information on the spatial distribution and optical/physical properties of the grains.

The fundamental goal of our research — to define the spatial distribution, the sinks and sources, the dynamics, and the physical description of the interplanetary grains — is a two-step process. The first step consists of observing and defining the *macroscopic features of the dust complex*. The second step (now in its beginning stages) is to use the physics of light scattering to derive the *microscopic features of the grains*. During this fourth year of AFOSR sponsorship, we have established step one firmly enough to be used as the stepping stone to step two. The accomplishments of the

last year in capstoning step one are briefly listed below. Some of the references cited therein are results of previous AFOSR sponsorship and are provided for completeness. Publications fully or partially supported by this contract are included as attachments.

SIGNIFICANT RESULTS

1. Background starlight over the sky. Pioneer 10/11 observations from beyond the asteroid belt, where the zodiacal light was found to be negligible, provided the *first* all-sky data on background starlight in the absence of the atmospheric radiations and zodiacal light. These two-color, all-sky data, now in the form of an Atlas, are a fundamental source of data for a number of fields in astronomy and astrophysics. (Schuerman, *et al.*, COSPAR 1977). Sample data are illustrated in a recent issue of *Sky and Telescope* (February 1981, attached), and the full body of data is being considered for use with a new edition of the well-known Atlas Coeli.

2. Inversion of the zodiacal light (ZL) brightness integral. The *general* inversion of the ZL brightness integral has been derived and is being used in our analysis of Pioneer ZL observations. It is also in use or planned for analysis of other ZL observations, ground-based or Earth-orbiting or space probe. This is a major tool and the only *complete* source of information on particle properties from photometric data. (Schuerman, *Bull. AAS*, 9, 564, 1977; Schuerman, *Planetary Space Sci.*, 27, 551, 1979; Schuerman, *Planet. Space Sci.*, 28, 1077, 1980.)

3. Properties of interplanetary dust beyond 1 AU. Our inversion of Pioneer 10/11 ZL data has found the first evidence that the properties of dust beyond 1 AU are *not* homogeneous — one of the *major* assumptions in most studies of the interplanetary dust complex. (Schuerman, in *Proc. IAU Symp. No. 90*, Halliday and McIntosh, eds., D. Reidel Publ. Co., Dordrecht, 25, 1980.)

4. The positions of maximum interplanetary dust density. Our analysis of ground and space observations of the photometric axis of zodiacal light has shown that there is no unique plane of "symmetry" or concentration for interplanetary dust, but rather a "multiplicity of planes" apparently

associated with the orbital planes of the planets. (Misconi and Weinberg, *Science*, 200, 1484, 1978; Misconi, in *Proc. IAU Symp. No. 90*, 49, 1980.

5. Asymmetries in the spatial distribution of interplanetary dust. As part of a study to include radiation pressure and the Poynting-Robertson effect in the classical restricted three-body problem, it was discovered that there might exist interplanetary dust arcs. This leads to a number of ramifications concerning sources and sinks for the interplanetary dust complex. (Schuerman, *Astrophys. J.*, 238, 337-342, 1980; Schuerman, in *Proc. IAU Symp. No. 90*, 285, 1980.

6. Ph.D. dissertations. Three theses have been completed:

   (1) G. N. Toller — A Study of Galactic Light, Extragalactic Light, and Galactic Structure Using Pioneer 10 Observations of Background Starlight (Space Astronomy Laboratory and SUNY Stony Brook).

   (2) R. Schaefer — Calculations of the Light Scattered by Randomly Oriented Ensembles of Spheroids of Size Comparable to the Wavelength (Space Astronomy Laboratory and SUNY Albany).

   (3) B. Å. S. Gustafson — Scattering by Ensembles of Small Particles: Experiment, Theory, and Application (Space Astronomy Laboratory and University of Lund).

   Their abstracts are attached.

Measuring Background Starlight

J. L. WEINBERG,
Space Astronomy Laboratory

IMAGINE EYES so poor that they can't resolve four moons side by side, but eyes so fortunate that they can see the sky liberated not only from contaminating smog and airglow, but also from the zodiacal light and even bright stars.

Such a vista of the cosmic background light has been derived from data gathered by Pioneers 10 and 11 as they sped to and beyond Jupiter. Aboard these interplanetary probes were photopolarimetric eyes from the University of Arizona that periodically mapped the sky brightness in blue and red light. Pioneer 10 made 76 full or partial scans between March, 1972, and February, 1976; its twin yielded 67 starting in April, 1973.

Since so many scans are available, several can be combined to portray more accurately the cosmic glow. The red lines on these pages combine readings from six maps by Pioneer 10. The light contributed by foreground stars — more or less those plotted on the base map — was subtracted before the contours were drawn.

Looking outward from the solar system, the Pioneers revealed that the sky brightness remained constant once the dusty space interior to the asteroid belt had been passed; that is, the zodiacal light became negligible relative to the background starlight. All that remained was the glow from faint stars, our galaxy, and sources beyond.

The base map, Chart 16 in the *Atlas of the Heavens*, shows about 1/15 of the sky centered on the south celestial pole. Pale and deep blue shadings indicate, respectively, dim and bright regions of the Milky Way. At top center is the Large Magellanic Cloud; its congener lies to the lower right. Dark nebulae are depicted as gray patches.

The interval between isophotes (contours of constant brightness) is equivalent to the light of 10 10th-magnitude solar-color stars per square degree in the V (yellow) standard photometric band.

This research began at Dudley Observatory in 1969 and continued at the State University of New York at Albany from 1973. Last year the activities and staff affiliated with the Department of Astronomy, University of Florida, 1810 NW 6th St., Gainesville, Fla. 32601. For further information, write the author at that address.

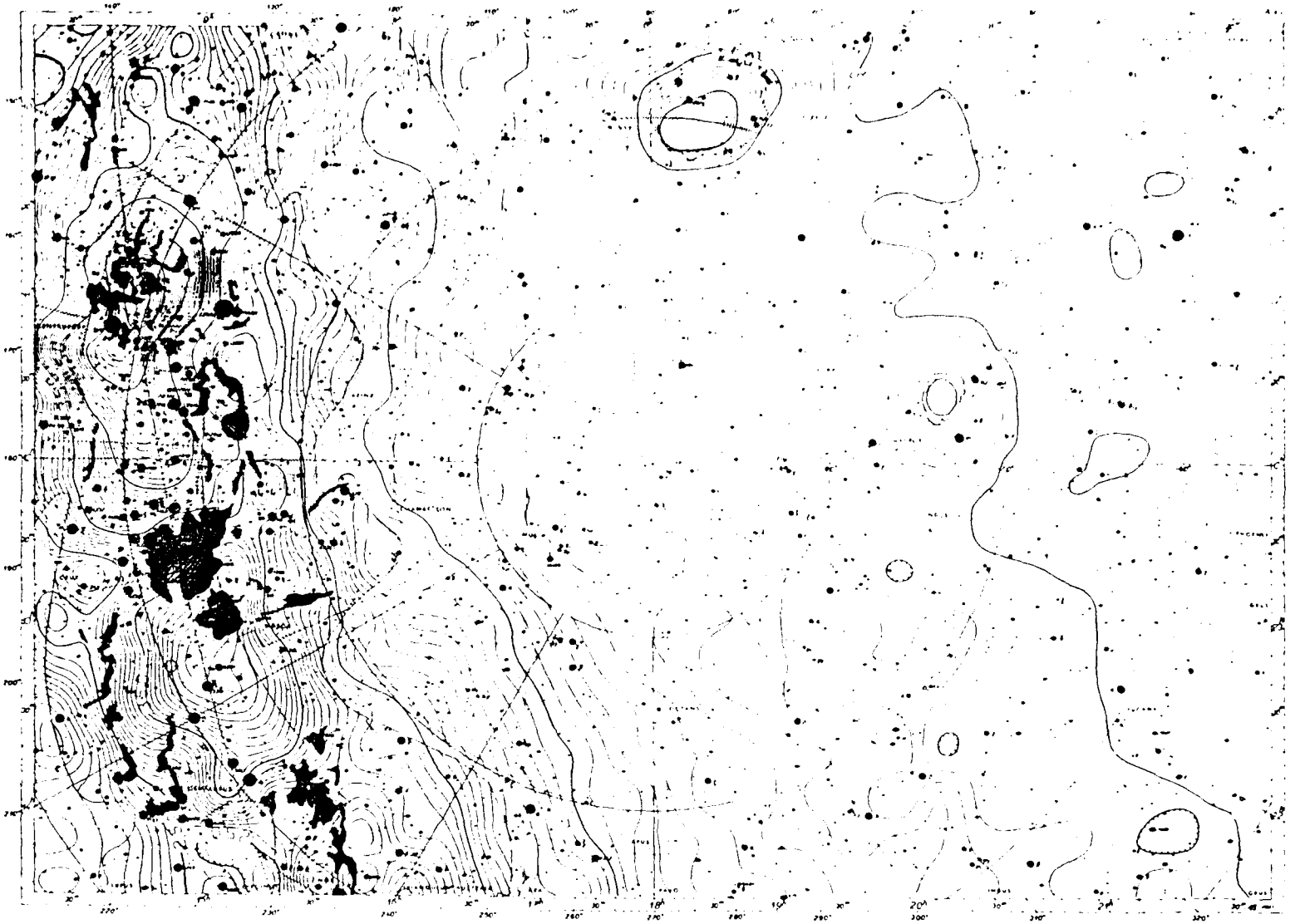

The red isophotal contours from Pioneer 10 and 11 data reveal the intrinsic brightness of the night sky, free from bright stars and light due to the Earth's atmosphere and interplanetary dust. The faintest stars shown are approximately of visual magnitude 7¼.

Maps such as this will allow astronomers to assess accurately the contributions to the brightness of the night sky from *terrestrial* and interplanetary sources. They will also permit a start at sorting out *the components of the background* starlight itself. It is instructive to compare the isophotal contours with wide-angle photographs, such as on pages 436 and 437 of the June, 1977, issue.

THE ASTROPHYSICAL JOURNAL, 238:337–342, 1980 May 15

THE RESTRICTED THREE-BODY PROBLEM INCLUDING RADIATION PRESSURE

DONALD W. SCHUERMAN
Space Astronomy Laboratory, State University of New York at Albany
Received 1979 September 14, accepted 1979 November 14

ABSTRACT

The classical restricted three-body problem is generalized to include the force of radiation pressure and the Poynting-Robertson effect. The positions of the Lagrangian points L_4 and L_5 are found as functions of β, the ratio of radiation to gravitational forces. The Poynting-Robertson effect renders the L_4 and L_5 points unstable on a time scale (T) long compared to the period of rotation of the two massive bodies. For the solar system, T is given by $T \approx [(1-\beta)^{2.5}\beta]544a^2$ yr, where a is the separation between the Sun and the planet in AU. Implications for space colonization and a mechanism for producing azimuthal asymmetries in the interplanetary dust complex are discussed; testing the latter may be possible by using the zodiacal light photopolarimeter aboard the *International Solar Polar Mission* spacecraft to be launched in 1983.

Subject headings: interplanetary medium — solar system: general — stars: stellar dynamics

I. INTRODUCTION

In an earlier paper (Schuerman 1972) the effect of radiation pressure on the effective gravitational potential in the restricted three-body problem was investigated. If one component of a binary system is very luminous ($\sim 10^4\ L_\odot$), it was shown that the familiar "contact surface" may not exist and the atmosphere of the brighter component has access to a much larger region of space than that predicted by the classical Roche potential. In this study, the restricted three-body problem, modified to include the force due to radiation, is investigated with respect to the location and stability of the resulting equilibrium points, L_i ($i = 1-5$). At these points the net force is zero. The locations of the equilibrium points are determined by the ratio (β) of the force due to radiation pressure to the force due to gravitation acting on a mass m of radiation pressure cross section σ_ν:

$$\beta = \frac{\int L_\nu \sigma_\nu d\nu}{4\pi c G M m}. \tag{1}$$

L_ν is the luminosity in the frequency range ν to $\nu + d\nu$ of a star of mass M; the other symbols have their usual meanings. The radiation pressure cross section may be written AQ_ν, where A is the geometric cross section and Q_ν is a dimensionless "efficiency factor" which is a function of particle size, shape, and optical properties. For a star of mass M and luminosity $L \equiv \int L_\nu d\nu$, β is roughly determined by the ratio of A to m for particle sizes larger than or equal to the wavelength of the incident radiation. Schwehm (1976), for example, shows that β is of the order unity for interplanetary particles whose radii are between 0.1 and 1 μm.

Spacecraft and artificial satellites can now be manufactured with $m \gg A$ such that $\beta \approx 1$ for these larger structures. (An extreme example is that of "solar sails" which could utilize radiation pressure to power spacecraft through the solar system.) The term β particle applies here to either a small particle or an artificial body situated near the Sun or a star such that β is nonnegligible.

The inclusion of the force of radiation pressure in the restricted three-body problem is presented here in two steps. First, the major radial components of the pressure force are considered for the case of a β-particle in the vicinity of *two luminous*, massive bodies. The two possibly-stable Lagrangian points, L_4 and L_5, are shown not to be confined to their familiar triangular positions. Depending upon the values of β, L_4 and L_5 may be located anywhere within the union of two circles which are centered on the two stars and which have equal radii corresponding to the separation of the two stars. Since β is a function of particle size, so are the equilibrium positions of individual particles. A stability criterion, which reduces to that of the classical problem in the case $\beta \to 0$, is derived. In the second step, the Poynting-Robertson effect is introduced for the case of *one luminous* body. This first-order relativistic effect does not significantly change the positions of L_i, but renders the L_4 and L_5 points unstable on time scales long compared to the period of revolution of the two massive bodies.

II. SOLUTION WITH RADIATION PRESSURE

In the restricted three-body problem, a steady state solution is sought for the motion of a test particle in the gravitational field of two larger, orbiting bodies of masses M_1 and M_2. It is assumed that M_1 and M_2 are in circular

orbits about their common center of mass and that their angular frequency (Ω) is given by $\Omega^2 = G(M_1 + M_2)/a^3$ where a, the distance between mass centers, is used as the unit of length. It is further assumed that the test particle remains in the plane in which M_1 and M_2 revolve. In the rotating reference frame (see Fig. 1) whose origin is the center of mass and whose angular frequency is Ω, the two components of the equation of motion of a β-particle with coordinates (X, Y) are

$$\frac{\ddot{X}}{\Omega^2} - \frac{2\dot{Y}}{\Omega} = X - \frac{(1-\beta_1)\mu(X+\mu-1)}{r_1^3} - \frac{(1-\beta_2)(1-\mu)(X+\mu)}{r_2^3}, \tag{2}$$

$$\frac{\ddot{Y}}{\Omega^2} + \frac{2\dot{X}}{\Omega} = \left[1 - \frac{(1-\beta_1)\mu}{r_1^3} - \frac{(1-\beta_2)(1-\mu)}{r_2^3}\right]Y. \tag{3}$$

M_2 is located at $X = 1 - \mu$, M_2 is located at $X = -\mu$, and $\mu = M_1/(M_1 + M_2)$. The distances from the point (X, Y) to the centers of mass M_1 and M_2 are $r_1 = [(X+\mu-1)^2 + Y^2]^{1/2}$ and $r_2 = [(X+\mu)^2 + Y^2]^{1/2}$, respectively. The two terms on the left-hand sides of equations (2) and (3) represent the acceleration and the Coriolis force experienced by the β-particle. The centrifugal acceleration has been placed on the right-hand sides (RHSs) of the equations because, like the remaining forces, it is a function of position only. The last two terms on the RHSs of equations (2) and (3) represent the components of the "effective" gravitational forces. These terms differ from those of the classical problem in that *each component has been reduced by a factor of the form* $1 - \beta$.

The equilibrium points L_4 and L_5 are found by setting the RHSs of equations (2) and (3) equal to zero with $Y \neq 0$. The resulting solution is

$$r_1 = (1-\beta_1)^{1/3} \equiv \delta_1, \qquad r_2 = (1-\beta_2)^{1/3} \equiv \delta_2, \tag{4}$$

or equivalently

$$X = \frac{1+\delta_2^2-\delta_1^2}{2} - \mu \equiv X_0, \qquad Y = \pm\delta_1\delta_2\left[1 - \left(\frac{\delta_1^2+\delta_2^2-1}{2\delta_1\delta_2}\right)^2\right]^{1/2} \equiv Y_0. \tag{5}$$

From solution (4) it follows that the L_4 and L_5 points exist only if all of the following conditions are satisfied:

$$\delta_1 + \delta_2 \geq 1, \qquad 0 < \delta_1 \leq 1 \text{ and } 0 < \delta_2 \leq 1. \tag{6}$$

These results are plotted in Figure 2 which shows the positions of the L_4 and L_5 points as a function of β_1 and β_2 (and, equivalently, δ_1 and δ_2). For $\delta_1 = \delta_2 = 1$, the classical triangular points are recovered. For all other values of δ_1 and δ_2 satisfying conditions (6), L_4 and L_5 are confined to the intersections of the two sets of circles given by equation (4). For the limiting case $\delta_1 + \delta_2 \to 1$, L_4, L_5, and the interior Lagrangian point L_1 all converge to the position $X = 1 - \delta_1 - \mu$, $Y = 0$. For $\delta_1 + \delta_2 < 1$, L_4 and L_5 have no solutions.

The *stability* of the equilibrium points is determined by investigating the motion resulting from a small displacement of the β-particle from its equilibrium position. If equations (2) and (3) are linearized with respect to small displacements of the form $X = X_0(1 + x)$ and $Y = Y_0(1 + y)$, the resulting linear equations admit solutions with an explicit time dependence of the form $x = x\exp(p\Omega t)$, $y = y\exp(p\Omega t)$. Equations (2) and (3) then become

$$X_0 x\left[p^2 - \frac{3\mu(X_0+\mu-1)^2}{\delta_1^5} - \frac{3(1-\mu)(X_0+\mu)^2}{\delta_2^5}\right] + Y_0 y\left[-2p - \frac{3\mu Y_0(X_0+\mu-1)}{\delta_1^5} - \frac{3(1-\mu)Y_0(X_0+\mu)}{\delta_2^5}\right] = 0, \tag{7}$$

$$X_0 x\left[2p - \frac{3\mu Y_0(X_0+\mu-1)}{\delta_1^5} - \frac{3(1-\mu)Y_0(X_0+\mu)}{\delta_2^5}\right] + Y_0 y\left[p^2 - \frac{3\mu Y_0^2}{\delta_1^5} - \frac{3(1-\mu)Y_0^2}{\delta_2^5}\right] = 0. \tag{8}$$

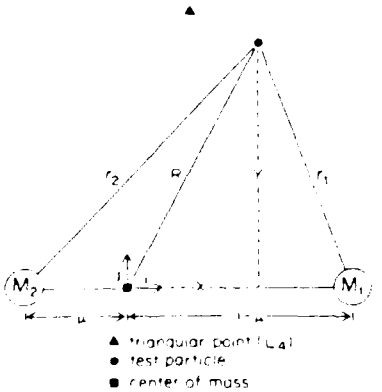

FIG. 1.—The coordinate system used in this study. This reference frame is noninertial; it rotates about the center of mass with angular frequency Ω.

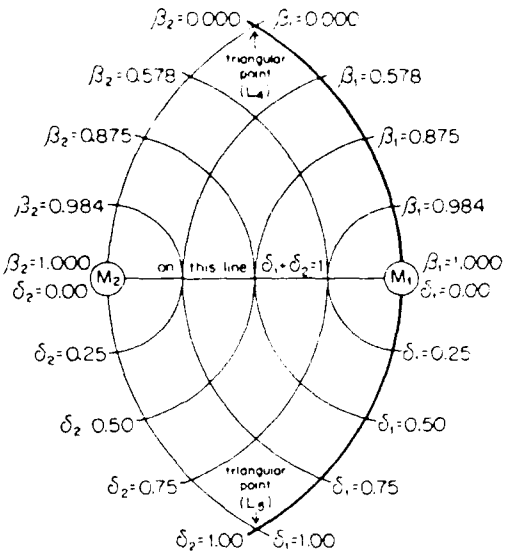

FIG. 2.—The possible positions of the equilibrium points L_4 (in upper half-plane) and L_5 (in lower half-plane) as a function of β_1 and β_2 or δ_1 and δ_2 [$\delta \equiv (1 - \beta)^{1/2}$]. The heavy line applies to systems with only *one* luminous body, M_1.

In order that the amplitudes $X_0 x$ and $Y_0 y$ be arbitrarily small, the determinant of this homogeneous set of equations must vanish; i.e., equations (7) and (8) must differ by only a constant factor. This restricts the possible values of p to the roots of the equation

$$p^4 + p^2 + 9\mu(1 - \mu)b = 0\,, \qquad \text{where } b \equiv 1 - \left(\frac{{\delta_1}^2 + {\delta_2}^2 - 1}{2\delta_1\delta_2}\right)^2. \tag{9}$$

These four ($n = 1$–4) roots,

$$p_n = \pm i\left[\tfrac{1}{2} \pm \left[\tfrac{1}{4} - 9\mu(1 - \mu)b\right]^{1/2}\right]^{1/2}, \tag{10}$$

determine the normal modes of the linearized system. In order that the motion be stable, *none* of the p_n's can contain a positive, real part which would thus lead to an $\exp(p\Omega t)$ increase in the motion of the β-particle. From equation (10) it follows that the motion is stable provided that

$$1 \geq 36\mu(1 - \mu)b\,. \tag{11}$$

Lagrange's classical criterion for stability is recovered in the limit of no radiation pressure ($\delta_1 \to 1$, $\delta_2 \to 1$; $b \to \frac{3}{4}$) for which equation (11) becomes

$$1 \geq 27\mu(1 - \mu) \qquad \text{or} \qquad [(1 - \mu) \text{ or } \mu] \geq 0.96148\,. \tag{12}$$

The greatest restriction on μ occurs for the case $({\delta_1}^2 + {\delta_2}^2) \to 1$ for which equation (11) reduces to

$$1 \geq 36\mu(1 - \mu) \qquad \text{or} \qquad [(1 - \mu) \text{ or } \mu] \geq 0.97140\,. \tag{13}$$

Thus, although radiation pressure produces a large effect on the location of the L_4 and L_5 points, it has a very small effect on restricting the values of μ necessary for stability (as formulated in this section).

A similar analysis can be carried out for the equilibrium points L_1, L_2, and L_3 for which $Y = 0$ in equations (2) and (3). It is found that, as in the classical case, these points are unstable and no equilibrium points exist for $\beta_1 > 1$ or $\beta_2 > 1$. The sole exception to this result is the degenerate case for which $(\delta_1 + \delta_2) \to 1$: then L_1—the interior Lagrangian point—and L_4 and L_5 all converge to the same point on the X axis ($1 - \delta_1 - \mu$), and that point is stable for all values of μ.

It is of interest to consider the implications of these results for the solar system. The subscript 1 then refers to the Sun while subscript 2 refers to a planet. In this case β_2 vanishes, δ_2 is unity, and the subscripts on β_1 and δ_1 are dropped for convenience (here and throughout the rest of this paper). Submicron particles have values of β which can be an appreciable fraction of unity. Such particles *cannot* be "trapped" at the classical triangular points as are the Trojan planets of the Sun-Jupiter system. Even if other forces (e.g., Lorentz, Poynting-Robertson) are not considered, the classical triangular points are *not* equilibrium points for these small particles. Their equilibrium points lie on the arc of a circle which is centered on M_2 and whose radius is the distance separating the Sun and M_2. This arc is shown as the heavy curve in Figure 2. The location of the equilibrium points on this arc are parametrized by β. As $\beta \to 1$ the L_4 and L_5 points approach the center of the Sun. If no other forces are considered, this

mechanism could act like a size or mass spectrometer; a distribution of small particles arranged according to their β values as shown in Figure 2 would be maintained for an arbitrarily long time. In the next section, the Poynting-Robertson force due to one body is taken into account. When this force is considered, the L_4 and L_5 points are found to be unstable on time scales long compared to Ω^{-1}.

The results mentioned thus far have an interesting application for artificial satellites and future space colonization. It has been suggested (e.g., O'Neill 1974) that the classical triangular points of the Sun-Jupiter or Sun-Earth system would be convenient sites to locate future space colonies. Such colonies would presumably mine asteroids for at least some of their raw materials. Present day technology permits the construction of spacecraft whose value of β can be made or varied in the range $0 \leq \beta < 1$. (A spacecraft with $\beta > 1$ has been considered by NASA as a "sailing" vehicle for chasing Halley's comet [Friedman 1976].) A space colony with a solar-facing adjustable "sail" could thus "park" (i.e., remain stationary with respect to the Sun and a planet without expending large amounts of energy) not only at the classical positions but at any heliocentric distance out to that of the planet.

III. THE POYNTING-ROBERTSON CORRECTION

Poynting (1903) was the first to suggest that β-particles in solar orbit suffer a gradual loss of angular momentum and ultimately spiral into the Sun. In a system of coordinates where the Sun is at rest, radiation scattered by the β-particle in the direction of motion suffers a blueshift, and in the opposite direction it is redshifted. This gives rise to a net drag force which opposes the direction of motion. The proper relativistic treatment of this problem was formulated by Robertson (1937) who showed that to first order in V/c, the radiation pressure force is given by

$$\boldsymbol{P} = \frac{\beta GM}{a^2 r_1^2}\left[\boldsymbol{r}_1 - \frac{(\boldsymbol{V}\cdot\boldsymbol{r}_1)\boldsymbol{r}_1}{r_1^2} - \frac{\boldsymbol{V}}{c}\right]. \tag{14}$$

The zero-order term has been treated in the preceding sections. The second term on the right-hand side of equation (14) represents the Doppler shift of the incident radiation, and the last term is the Poynting drag. These last two terms taken together are the effect under consideration.

To incorporate the Poynting-Robertson force into the restricted three-body problem as formulated in the preceding section, the velocity vector $\boldsymbol{V}$ of the β particle must be transformed to the rotating system centered on the center of mass:

$$\boldsymbol{V} = \boldsymbol{v} + \boldsymbol{\Omega}\cdot\mathbf{R}, \qquad \boldsymbol{v} = \dot{X}\boldsymbol{i} + \dot{Y}\boldsymbol{j}, \tag{15}$$

where $\boldsymbol{i}$ and $\boldsymbol{j}$ are unit orthogonal vectors in the rotating frame (see Fig. 1). In dimensionless units the $\boldsymbol{i}, \boldsymbol{j}$ components of the Poynting-Robertson force can then be incorporated into equations (2) and (3) so that

$$\ddot{X} - 2\Omega\dot{Y} - \Omega^2 X = \left[\frac{\dot{X}}{\Omega c}(X+\mu-1) + \frac{\dot{Y}}{\Omega c}Y\right](X+\mu-1)\left\{\frac{\delta^3\mu}{r_1^2}\right\} = -\frac{\delta^3\mu(X+\mu-1)}{r_1^3} - \frac{(1-\mu)(X+\mu)}{r_2^3} + X - \frac{\gamma\dot{Y}}{r_1^2}, \tag{16}$$

$$\ddot{Y} + 2\Omega\dot{X} - \Omega^2 Y = \left[\frac{\dot{X}}{\Omega c}(X+\mu-1) + \frac{\dot{Y}}{\Omega c}Y\right]Y\left\{\frac{\delta^3\mu}{r_1^2}\right\} = -\frac{\delta^3\mu Y}{r_1^3} - \frac{(1-\mu)Y}{r_2^3} + Y - \frac{\gamma(\dot{X}+\mu-1)}{r_1^2}, \tag{17}$$

where γ, which contains the parameter analogous to V/c, is given by $\gamma \equiv \beta\mu a\Omega/c$. The positions of the L_4 and L_5 points are, once again, found by setting the RHSs of equations (16) and (17) equal to zero with $Y \neq 0$. To first order in γ, the solution is

$$r_1 = \delta\left(1 + \frac{\gamma}{6\mu Y_0}\right), \qquad r_2 = 1 + \frac{\gamma}{3(1-\mu)Y_0}, \tag{18}$$

or equivalently,

$$X = X_0\left\{1 - \frac{\gamma[\mu + (1-\mu)\delta^2/2]}{3(1-\mu)Y_0 X_0}\right\} \equiv X_0, \tag{19}$$

$$Y = Y_0\left\{1 - \frac{\gamma\delta^2[\mu - (1-\mu)(1-\delta^2/2)]}{6\mu(1-\mu)Y_0^3}\right\} \equiv Y_0. \tag{20}$$

X_0 and Y_0 represent the equilibrium positions of the L_4 and L_5 points when the Poynting-Robertson effect is not included and when $\beta_2 = 0$, $\delta_2 = +1$ in equations (5):

$$X_0 = 1 - \mu - \delta^2/2, \qquad Y_0 = \pm\delta(1 - \delta^2/4)^{1/2} \neq 0. \tag{21}$$

Equations (18)–(20) are valid provided the first order terms in γ are small compared to unity.

The stability of the steady state solution derived above is analyzed by the same technique as that used in § II.

Equations (16) and (17) are linearized with respect to small displacements about the equilibrium points, L_4 and L_5, given by equation (19) and (20):

$$X = X_0'[1 + x \exp(p\Omega t)], \qquad Y = Y_0'[1 + y \exp(p\Omega t)]. \tag{22}$$

A straightforward calculation yields the result, analogous to equations (7) and (8), that

$$X_0'x\left\{p^2 + \frac{\gamma p}{\delta^2}\left[1 + \frac{(X_0' + \mu - 1)^2}{\delta^2}\right] + \frac{\delta^3\mu}{r_1^3}\left[1 - \frac{3(X_0' + \mu - 1)^2}{r_1^2}\right] + \frac{(1-\mu)}{r_2^3}\left[1 - \frac{3(X_0' + \mu)^2}{r_2^2}\right] - 1 + \frac{2\gamma Y_0'(X_0' + \mu - 1)}{\delta^4}\right\}$$

$$- Y_0'y\left[-2p + \frac{\gamma Y_0'(X_0' + \mu - 1)p}{\delta^4} - \frac{3\delta^3\mu Y_0'(X_0' + \mu - 1)}{r_1^5} - \frac{3(1-\mu)Y_0'(X_0' + \mu)}{r_2^5} - \frac{\gamma}{\delta^2} + \frac{2\gamma Y_0'^2}{\delta^4}\right] = 0, \tag{23}$$

$$X_0'x\left[2p + \frac{\gamma Y_0'(X_0' + \mu - 1)p}{\delta^4} - \frac{3\delta^3\mu Y_0'(X_0' + \mu - 1)}{r_1^5} - \frac{3(1-\mu)Y_0'(X_0' + \mu)}{r_2^5} - \frac{2\gamma(X_0' + \mu - 1)^2}{\delta^4} + \frac{\gamma}{\delta^2}\right]$$

$$- Y_0'y\left\{p^2 - \frac{\gamma p}{\delta^2}\left(1 + \frac{Y_0'^2}{\delta^2}\right) + \frac{\delta^3\mu}{r_1^3}\left[1 - \frac{3(Y_0')^2}{r_1^2}\right] + \frac{(1-\mu)}{r_2^3}\left[1 - \frac{3(Y_0')^2}{r_2^2}\right] - 1 - \frac{2\gamma Y_0'(X_0' + \mu - 1)}{\delta^4}\right\} = 0. \tag{24}$$

For a solution to exist, the determinant of this set of linear, homogeneous equations must vanish. This yields a fourth order equation in p of the form

$$(1 + a_4)p^4 + a_3p^3 + (1 + a_2)p^2 + a_1p + 9\mu(1-\mu)b(1 - a_0) = 0, \tag{25}$$

where b, defined in equation (9), reduces to $b = 1 - \delta^2/4$ and a_j ($j = 0, 1, \ldots, 4$) must be first order terms in γ. We seek a solution of equation (25) of the form $p = p_n(1 + \alpha + i\eta)$ where p_n is given by equations (10), restrictions (11) applies, and both α and η must be first order terms in γ. Then p takes the form

$$p = \pm i(1 + \alpha)[\tfrac{1}{2} \pm (\tfrac{1}{4} - 9\mu(1-\mu)b)^{1/2}]^{1/2} \mp \eta[\tfrac{1}{2} \pm (\tfrac{1}{4} - 9\mu(1-\mu)b)^{1/2}]^{1/2}. \tag{26}$$

Thus, if the β particle is displaced from its equilibrium position, it will oscillate with frequencies determined by the imaginary part of p in equation (26) while the *growth in the amplitude* of those oscillations is determined by the real part of p. It is the time scale of the latter that will be investigated here. If equation (26) is substituted into equation (25), the following expression for η is obtained:

$$\eta = \pm\frac{[\tfrac{1}{2} \pm (\tfrac{1}{4} - 9\mu(1-\mu)b)^{1/2}]^{1/2}\{a_3[\tfrac{1}{2} \pm (\tfrac{1}{4} - 9\mu(1-\mu)b)^{1/2}] - a_1\}}{\pm 4(\tfrac{1}{4} - 9\mu(1-\mu)b)^{1/2}[\tfrac{1}{2} \pm (\tfrac{1}{4} - 9\mu(1-\mu)b)^{1/2}]}. \tag{27}$$

To evaluate η, it is only required that a_3 and a_1 (the coefficients of p^3 and p) be computed rather than the entire determinant of the set of equations (23) and (24). To first order in γ, we find

$$a_3 = \frac{3\gamma}{\delta^2}, \qquad a_1 = -\frac{3\gamma}{\delta^2}\left[1 + \frac{Y_0'^2(1-\mu)}{\delta^2}\right], \tag{28}$$

so that the e-folding time (T) for the growth of β-particle oscillations about the equilibrium points L_4 and L_5 is given by

$$\frac{1}{T} = \Omega\,\mathrm{Re}(p) = \frac{\gamma\Omega}{4\delta^2}\left[\frac{3\{\tfrac{1}{2} \pm [\tfrac{1}{4} - 9\mu(1-\mu)(1-\delta^2/4)]^{1/2}\} + 3[1 + (1-\mu)(1-\delta^2/4)]}{\pm[\tfrac{1}{4} - 9\mu(1-\mu)(1-\delta^2/4)]^{1/2}}\right]. \tag{29}$$

Under restriction (11), T is always positive for at least one choice of mode (sign) in equation (29). Therefore, β-particles in general have *no stable* equilibrium solutions of the restricted three-body problem if the Poynting-Robertson effect is taken into consideration.

T takes a more convenient form when applied to the solar system. For all of the planets including Jupiter, terms which contain the factor $(1 - \mu)$ can be ignored in equation (29). The mode with the smallest characteristic time (the fastest growing oscillation) has

$$T = \frac{\delta^2}{3\Omega\gamma} = \frac{(1-\beta)^{2/3}ca^2}{3\beta M_\odot G} \approx \frac{(1-\beta)^{2/3}}{\beta} 544a^2\ \mathrm{yr} \quad (a\ \mathrm{in\ AU}). \tag{30}$$

A convenient and representative value for β of 0.57 makes $(1 - \beta)^{2/3}/\beta = 1$. Thus, for example, the Sun-Jupiter

system ($a = 5.2$ AU) results in $T \approx 14,700$ yr. This means that if a particle with $\beta = 0.57$ is displaced slightly from its equilibrium position, it will oscillate about that position in some linear combination of its four normal modes and the amplitude of that motion will increase by a factor of e in 14,700 yr.

IV. DISCUSSION

It is not at all evident that the above mechanism could lead to a significant increase in the density of interplanetary β-particles along the arc schematically shown as a heavy line in Figure 2. Other forces act on these β-particles which cannot be treated by the analytical methods employed here. Interactions with the gravitational fields of intervening planets could displace some of the β-particles far enough from their equilibrium positions that the Coriolis force is insufficient to restore them. This effect would leave large gaps in the arc of β-particles. Jupiter, because of its great mass, would be particularly effective in disrupting the dust in arcs associated with the other planets; conversely, dust in the Sun-Jupiter arc would be the least affected by planetary encounters. The Lorentz force due to the solar magnetic field also acts on (charged) β-particles. This conservative force is roughly 40% that of the solar gravitation (Greenberg and Schuerman 1978). The uncertainties in the charges of the β-particles and in the long term fluctuations and reversals of the solar magnetic field at distances greater than 1 AU make the inclusion of the Lorentz force in this problem particularly difficult. Finally, the ions in the solar wind impinging on the β-particles and the Coulomb interaction between solar wind electrons and the β-particles contribute nonconservative drag forces which together are estimated to be about 30% of the Poynting-Robertson effect (Bandermann 1967; Misconi 1976*a*). These forces must surely operate to shorten the time scales (T) in equation (30).

Even if the planetary encounters do not disrupt the dust along the entire arc, and even if the large but conservative Lorentz force averages out to a small effect over many solar cycles, there still remains the need for a replenishment mechanism if an increase in the density of β-particles along a planetary arc is to be expected on a "steady state" basis. The major source of replenishment for the interplanetary dust complex is thought to be cometary debris (Whipple 1955, 1967; Dohnanyi 1970, 1972, 1973). Comets shed both β-particles (some with $\beta > 1$) and larger particles; light scattering by the latter is the main contribution to the zodiacal light. These larger particles ultimately fragment through self-collisions (Zook 1975) or possibly by rotational bursting (Paddack and Rhee 1975; Misconi 1976*b*). It is not evident whether or not these sources of β-particles provide a wide enough distribution in real space and velocity space to deposit a significant fraction of "zero-velocity" β-particles at their appropriate equilibrium positions in times short compared to T in equation (30).

Mechanisms which tend to produce azimuthal asymmetries in the interplanetary dust complex are of great interest because present methods of inverting spacecraft observations of the zodiacal light (Dumont 1973; Schuerman 1979) depend upon the assumption of axial symmetry for the dust cloud. Fortunately, the International Solar Polar Mission whose launch is scheduled for 1983 February provides the opportunity to assess this assumption directly. A photopolarimeter (jointly designed by teams at the Ruhr-University, Bochum, FRG, and the State University of New York at Albany) will map the brightness and polarization of the zodiacal light throughout the 4½ year mission to Jupiter and back over (under) the poles of the Sun. During the two periods of solar polar passage, the spacecraft will be in the center of the solar system but at 1.7 AU above (and below) the ecliptic plane. From these vantage points, isophotes of the zodiacal light will appear as circles *only if* the interplanetary dust complex is truly azimuthally symmetric. In particular, gross enhancements in the spatial density of the dust along arcs associated with planets should be detectable. Furthermore, this study predicts that any diffuse light associated with the *classical* libration (L_4 and L_5) points of the planet-Sun systems must be due to grains larger than about a micron because the triangular points are *not* equilibrium points for β-particles.

This work was supported by the Air Force Office of Scientific Research (contract F49620-78-C-0013) and by the National Aeronautics and Space Administration (JPL contract 955137).

REFERENCES

Bandermann, L. W. 1967, Ph.D. thesis, University of Maryland.
Dohnanyi, J. S. 1970, *J. Geophys. Res.*, **75**, 3648.
———. 1972, *Icarus*, **17**, 1.
———. 1973, in *Evolutionary and Physical Properties of Meteoroids*, ed. Hemenway, Millman, and Cooks (Washington: NASA SP 319), p. 363.
Dumont, R. 1973, *Planet. Space Sci.*, **21**, 2149.
Friedman, L. D. 1975, in *Proceedings of the Shuttle-Based Cometary Science Workshop*, ed. G. A. Gary and K. S. Clifton (Huntsville: NASA Marshall Space Flight Center), p. 251.
Greenberg, J. M., and Schuerman, D. W. 1978, *Nature*, **275**, 39.
Misconi, N. Y. 1976*a*, *Astr. Ap.*, **51**, 357.
———. 1976*b*, *Geophys. Res. Letters*, **3**, 585.
O'Neill, G. K. 1974, *Phys. Today*, **27**, 32.
Paddack, S. J., and Rhee, J. W. 1975, *Geophys. Res. Letters*, **2**, 365.
Poynting, J. H. 1903, *Phil. Trans. Roy. Soc. A*, **202**, 525.
Robertson, H. P. 1937, *M.N.R.A.S.*, **97**, 423.
Schuerman, D. W. 1972, *Ap. Space Sci.*, **19**, 351.
——— 1979, *Planet. Space Sci.*, **27**, 551.
Schwehm, G. 1975, in *Lecture Notes in Physics*, Vol. **48**, ed. H. Elsasser and H. Fechtig (Heidelberg: Springer-Verlag), p. 459.
Whipple, F. L. 1955, *Ap. J.*, **121**, 750.
——— 1967, in *The Zodiacal Light and the Interplanetary Medium*, ed. J. L. Weinberg (Washington: NASA SP 150), p. 409.
Zook, H. A. 1975, *Planet. Space Sci.*, **23**, 1391.

DONALD W. SCHUERMAN: Space Astronomy Laboratory, State University of New York at Albany, Executive Park East, Albany, NY 12203

THE PHOTOMETRIC CENTER OF THE GEGENSCHEIN

by

Nebil Y. Misconi

Space Astronomy Laboratory
University of Florida
1810 N.W. Sixth Street
Gainesville, Florida 32601

Seven Manuscript Pages
Five Figures
No Tables

ABSTRACT

Model calculations are used to evaluate two factors which determine the position of the photometric center of the Gegenschein: the increased scattering efficiency of the interplanetary dust near backscattering (scattering angles $\theta \sim 165^{o} - 180^{o}$), and the spatial density distribution of the dust. Computer-generated brightness contours are used to investigate which of these two factors dominates, using empirical scattering functions with *and without* a brightness enhancement in the backscattering region. It is found that the effect of the enhanced scattering of light by dust in the backscattering region overrides the effect of the spatial-density distribution of the dust. As a result, the photometric center should be observed at the antisolar point at all times, except possibly when the antisolar point is at its maximum displacement from the symmetry plane.

1. INTRODUCTION

The position of the photometric center (maximum brightness) of the Gegenschein has been thought to relate directly to the spatial density distribution of interplanetary dust in the region of the Gegenschein. From observations of the Gegenschein, Dumont (1965), Robley (1965), and Roosen (1968, 1970a, 1970b) found the photometric center to be close to the ecliptic plane. However, Tanabe (1964, 1965, 1980) and Wolstencroft and Rose (1967) found the photometric center displaced from the ecliptic plane and close to the invariable plane of the solar system. Earlier observations (1950's) showed similar displacements (Figure 1). Pioneer 10 and 11 observations (Weinberg *et al.*, 1973) showed beyond doubt that the Gegenschein arises from enhancement in the backscattering of interplanetary dust. The question then arises as to whether the position of the photometric center is directly related to the maximum dust density distribution. We would like to emphasize that there are two factors which determine the position of the photometric center: the increased scattering efficiency of the interplanetary dust near backscattering (scattering angles of approximately 165° to 180°) and the spatial density distribution of the dust. In other words, can the position of maximum brightness be at the antisolar point if the plane of maximum dust density does not contain this point? Computer-generated brightness contours are used to investigate this question using empirical scattering functions with *and without* a brightness en-

hancement in the backscattering region, thereby separating the effect of the increased brightness from the effect of the spatial density distribution. It will be shown later that the enhancement in the backscattering overrides the spatial density distribution of the dust in the region of the Gegenschein.

2. MODEL CALCULATION

Predictions were made earlier (Figure 1) of the displacement in the ecliptic latitude of the photometric center for the plane of maximum dust density (symmetry plane) at the invariable plane or at the orbital plane of Mars (Misconi, 1977). These predictions were based only on the effect of the spatial density distribution of the dust. Using ground-based observations of the Gegenschein (Figure 2) Dumont (1965) found the photometric center of the Gegenschein to be in the ecliptic plane and the photometric axis (locus of points of maximum brightness) to be near the invariable plane. Dumont's findings agree with our predictions at 15° east and west of the antisolar point (Misconi, 1977), but disagree with the predictions in Figure 1 (where the effect of enhanced backscattering of the dust was not evaluated). Using a computer code developed earlier by Hanner (Misconi and Hanner, 1975), an attempt was made to reproduce Dumont's observational map of the Gegenschein (Figure 3). This map was generated using Dumont's (1975) empirical scattering function, which he deduced from his Gegenschein brightness data.

To separate the effect of increased scattering efficiency of interplanetary dust near backscattering from the spatial density distribution of the dust, a computer-generated brightness contour map was made (Figure 4) using the empirical scattering function *without* a brightness enhancement in the backscattering region. The spatial density distribution above and below the ecliptic

plane was assumed to follow the fan model suggested by Leinert *et al.* (1976). The fan model was intended to serve as a good example, although there are several other models that have also been suggested (see, for example, Geise, 1972, and Leinert *et al.*, 1976). Choosing a specific model for the density distribution is not considered critical for the purpose of separating the two effects mentioned above. This follows from Figure 1, since the displacement in ecliptic latitude of the symmetry plane is small (2.5°) for the time of Dumont's observations (February 9), and the various models of the dust distribution do not differ significantly at small latitudes from the ecliptic. Figure 4 shows very clearly that if it were not for the effect of enhanced backscatter, the photometric center of the Gegenschein would be displaced from the antisolar point by nearly the same displacement of the symmetry plane.

The question now arises as to whether or not the photometric center continues to be seen at the antisolar point at all seasons, even during the maximum displacement of the symmetry plane from the ecliptic. As the displacement of the symmetry plane from the ecliptic increases, the decrease in the number density of the dust at the antisolar point becomes model dependent. Therefore, the answer in this case depends heavily on the actual spatial density distribution of the dust above and below the ecliptic plane. A computer-generated map (Figure 5) was made using the fan model mentioned earlier for a time when the antisolar point is at maximum

displacement in ecliptic latitude from the invariable plane (this corresponds to $\lambda_\odot \sim 350^\circ - 50^\circ$ and $\lambda_\odot \sim 170^\circ - 220^\circ$) i.e., during March, April, September, and October. Figure 5 shows that if one uses the fan model the photometric center will not be seen at the antisolar point; it will tend instead toward the same displacement from the ecliptic as the symmetry plane near the antisolar point. This also means that the effect of enhanced backscattering is no longer apparent.

3. DISCUSSION AND CONCLUSION

This study addresses the present confusion in published results on the position of the photometric center of the Gegenschein. The significance of the true position to our understanding of the dynamics of interplanetary dust has been discussed earlier (Misconi, 1977). It is concluded from our model calculations that: (a) The effect of the enhanced scattering of light by dust in the backscattering region ($\theta \sim 165^{\circ} - 180^{\circ}$) overrides the effect of the spatial-density distribution of the dust in this region; (b) Although the photometric center is observed near the antisolar point, this does not mean that the dust density reaches a maximum at that point, but rather that the density has a maximum at the symmetry plane; (c) As a result of (a), the photometric center should be observed at the antisolar point at all times, except possibly when the antisolar point is at maximum displacement from the symmetry plane. This possibility depends heavily on the dust distribution above and below the symmetry plane. Information on the actual nature of the dust distribution will be obtained by the zodiacal light/background starlight experiment using observations obtained during the International Solar Polar Mission (Schwehm *et al.*, 1981). Such information can verify or deny the possibility mentioned in (c). We also hope to obtain new brightness maps of the Gegenschein at different times of the year from Mt. Haleakala, Hawaii, to establish the relative positions of the photometric center and the symmetry plane of the Gegenschein at all seasons.

If future ground-based observations of the Gegenschein show the symmetry plane to be near the invariable plane at all seasons with the photometric center always at the antisolar point (in the ecliptic plane), then it is very likely that the dust seen in the region of the Gegenschein is affected gravitationally by Jupiter.

ACKNOWLEDGEMENTS

I would like to thank Dr. J. L. Weinberg for critically reviewing the manuscript. This research was supported by the Air Force Office of Scientific Research and the National Aeronautics and Space Administration (Planetary Atmospheres Program).

REFERENCES

Dumont, R. (1965). *Ann. Astrophys.* *28*, 265-320.

_____. (1975). *Astron. Astrophys.* *38*, 405-412.

Elsässer, H., and Siedentopf, H. (1957). *Z. Astrophys.* *44*, 2, 132-143.

Giese, R. H. (1972). Zodiacal light and interplanetary particle number densities. In *Space Research XII*, pp. 437-443. Akademie-Verlag, Berlin.

Gindilis, L. M. (1960). *Soviet Astron. AJ.* *3*, 1004-1006.

Hoffmeister, C. (1940). *Astron. Nachr.* *271*, 49-67.

Leinert, C., Link, H., and Pitz, E. (1976). *Astron. Astrophys.* *47*, 221-230.

Lillie, C. F. (1968). An empirical determination of the interstellar radiation field. Ph.D. Thesis, University of Wisconsin.

Misconi, N. Y. (1977). *Astron. Astrophys.* *61*, 497-504.

_____, and Hanner, M. S. (1975). *Planetary Space Sci.* *23*, 1329-1335.

Roach, R. E., and Rees, M. H. (1956). The absolute photometry of the Gegenschein. In *The Airglow and the Aurorae* (E. B. Armstrong and A. Dalgarno, Eds.), pp. 142-155. Pergamon Press, London and New York.

Robley, R. (1965). *Ann. Geophys.* *21*, 505-513.

Roosen, R. G. (1968). *Icarus.* *9*, 429.

_____. (1970a). The Gegenschein. Ph.D. Thesis, University of Texas.

_____. (1970b). *Icarus.* *13*, 184-201.

REFERENCES, cont'd.

Schwehm, G. H., Giese, R. H., Giovane, F., Schuerman, D. W., and Weinberg, J. L. (In press). Recent developments in space-borne zodiacal light photometry. In *Space Research*.

Tanabe, H. (1964). Photoelectric observations of the Gegenschein. Ph.D. Thesis, University of Tokyo.

_____. (1965). *Pub. Astron. Soc. Japan.* 17, 339-366.

_____, Takechi, A., and Miyashita, A. (1980). Photometric axis measurements of the zodiacal light at large elongations. In *IAU Symposium No. 90, Solid Particles in the Solar System* (I. Halliday and B. A. McIntosh, Eds.), pp. 45-48. Reidel Publishing Company, Dordrecht, Holland.

Weinberg, J. L., Hanner, M. S., Mann, H. M., Hutchison, P. B., and Fimmel, R. (1973). Observations of zodiacal light from the Pioneer 10 Asteroid-Jupiter probe. In *Space Research XIII* (M. J. Rycroft and S. K. Runcorn, Eds.), pp. 1187-1193. Akademie-Verlag, Berlin.

Wolstencroft, R. D., and Rose, L. J. (1967). *Astrophys. J.*, 147, 271-292.

FIGURE CAPTIONS

Fig. 1. Predicted positions of the photometric center of the Gegenschein, for planes of symmetry corresponding to the orbital plane of Mars (---) and the invariable plane (——). Observed positions of the photometric center are also shown.

Fig. 2. Isophote map of the Gegenschein obtained by Dumont at Tenerife on February 9, 1964 (Dumont, 1965).

Fig. 3. Computer-generated isophote map of the Gegenschein using Dumont's empirical scattering function (Dumont, 1975).

Fig. 4. Brightness contours of the Gegenschein generated with no enhancement in the backscattering region ($\theta \sim 165^{\circ} - 180^{\circ}$).

Fig. 5. Computer-generated brightness contours for times when the symmetry plane is near its maximum displacement from the ecliptic plane.

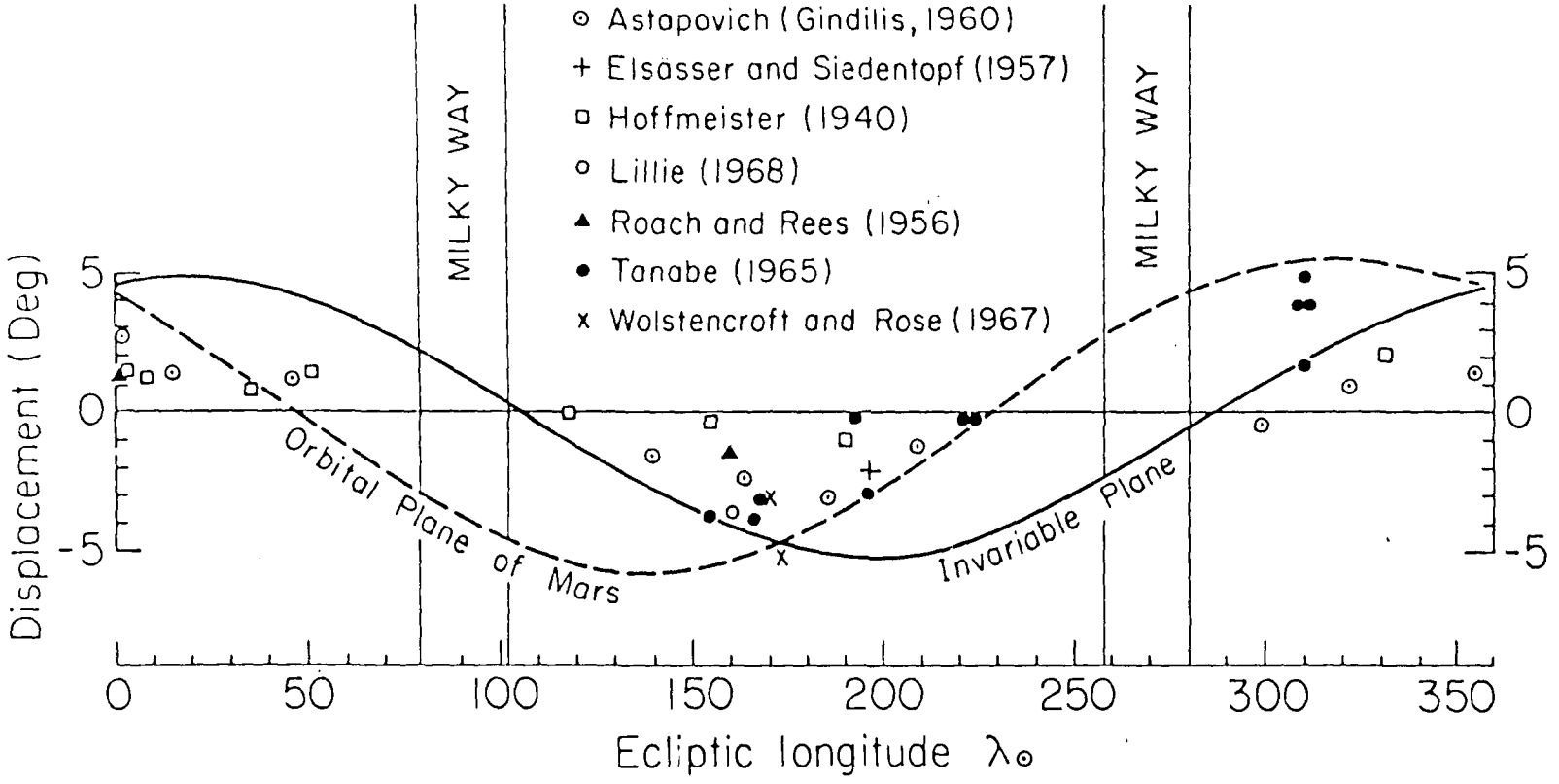
Astapovich (Gindilis, 1960)
Elsasser and Siedentopf (1957)
Hoffmeister (1940)
Lillie (1968)
Roach and Rees (1956)
Tanabe (1965)
Wolstencroft and Rose (1967)
MILKY WAY
MILKY WAY
Orbital Plane of Mars
Invariable Plane
Displacement (Deg)
5
0
-5
0
50
100
150
200
250
300
350
Ecliptic longitude λ⊙

Fig. 1

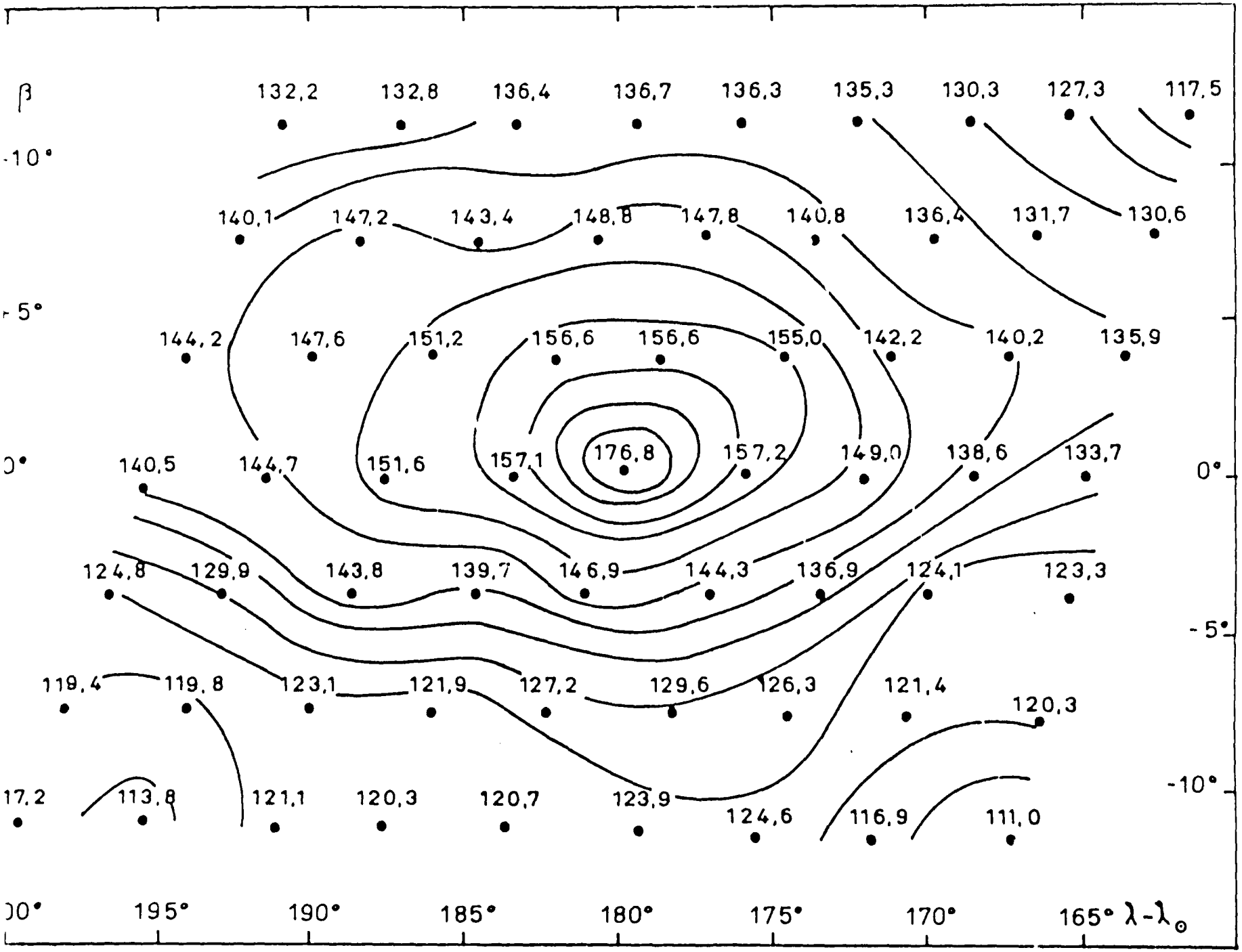
β
132,2
132,8
136,4
136,7
136,3
135,3
130,3
127,3
117,5
-10°
140,1
147,2
143,4
148,8
147,8
140,8
136,4
131,7
130,6
-5°
144,2
147,6
151,2
156,6
156,6
155,0
142,2
140,2
135,9
0°
140,5
144,7
151,6
157,1
176,8
157,2
149,0
138,6
133,7
0°
124,8
129,9
143,8
139,7
146,9
144,3
136,9
124,1
123,3
-5°
119,4
119,8
123,1
121,9
127,2
129,6
126,3
121,4
120,3
17,2
113,8
121,1
120,3
120,7
123,9
124,6
116,9
111,0
-10°
200°
195°
190°
185°
180°
175°
170°
165°
λ-λ⊙

Fig. 2

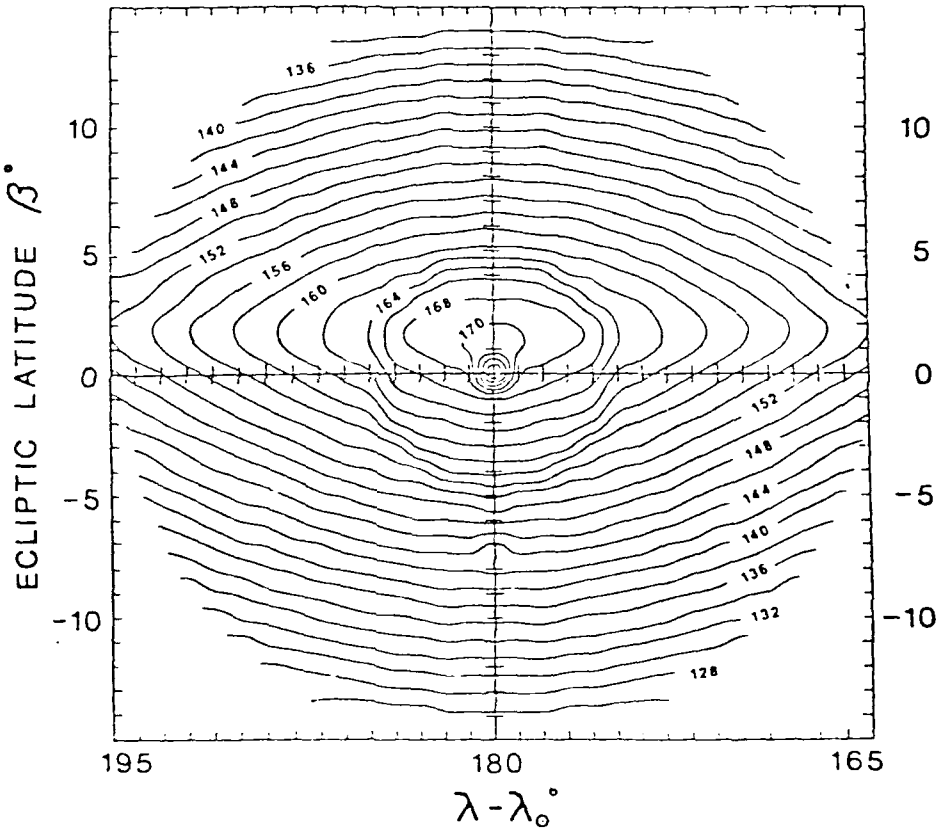
ECLIPTIC LATITUDE β°
10
5
0
-5
-10
136
140
144
148
152
156
160
164
168
170
152
148
144
140
136
132
128
195
180
165
λ-λ₀°
DIFFERENTIAL ECLIPTIC LONGITUDE

Fig 3

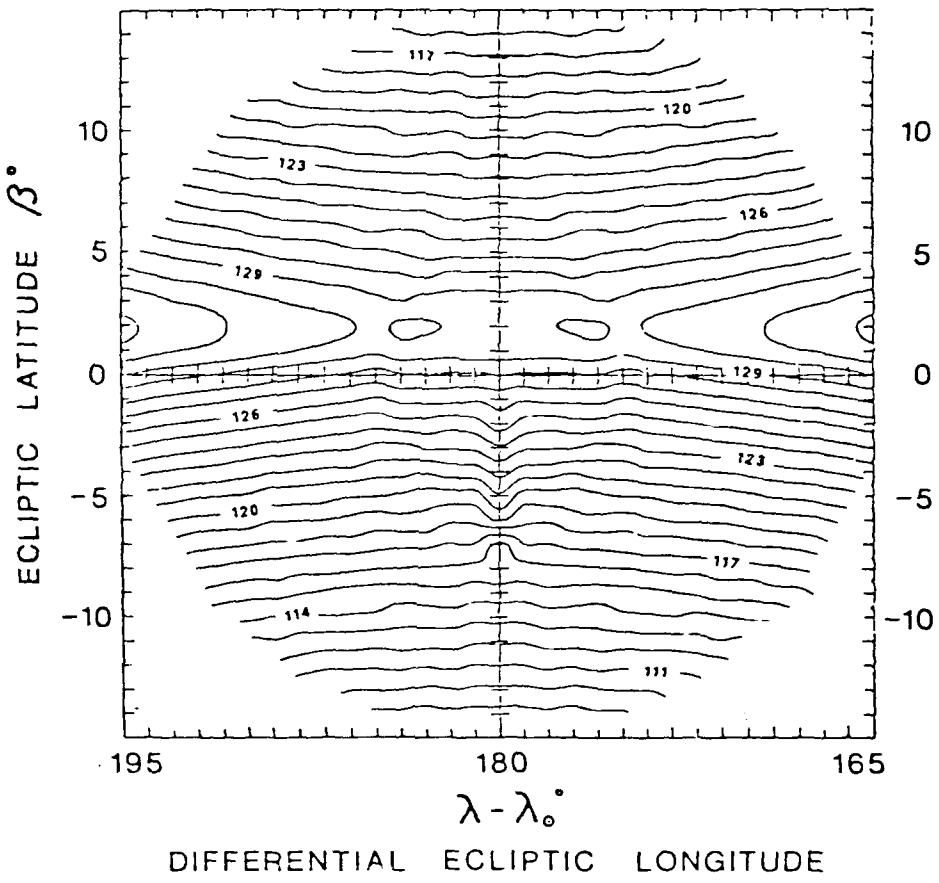
ECLIPTIC LATITUDE β°
10
5
0
-5
-10
117
120
123
126
129
129
126
123
120
117
114
111
195
180
165
λ - λ₀°
DIFFERENTIAL ECLIPTIC LONGITUDE

Fig. 4

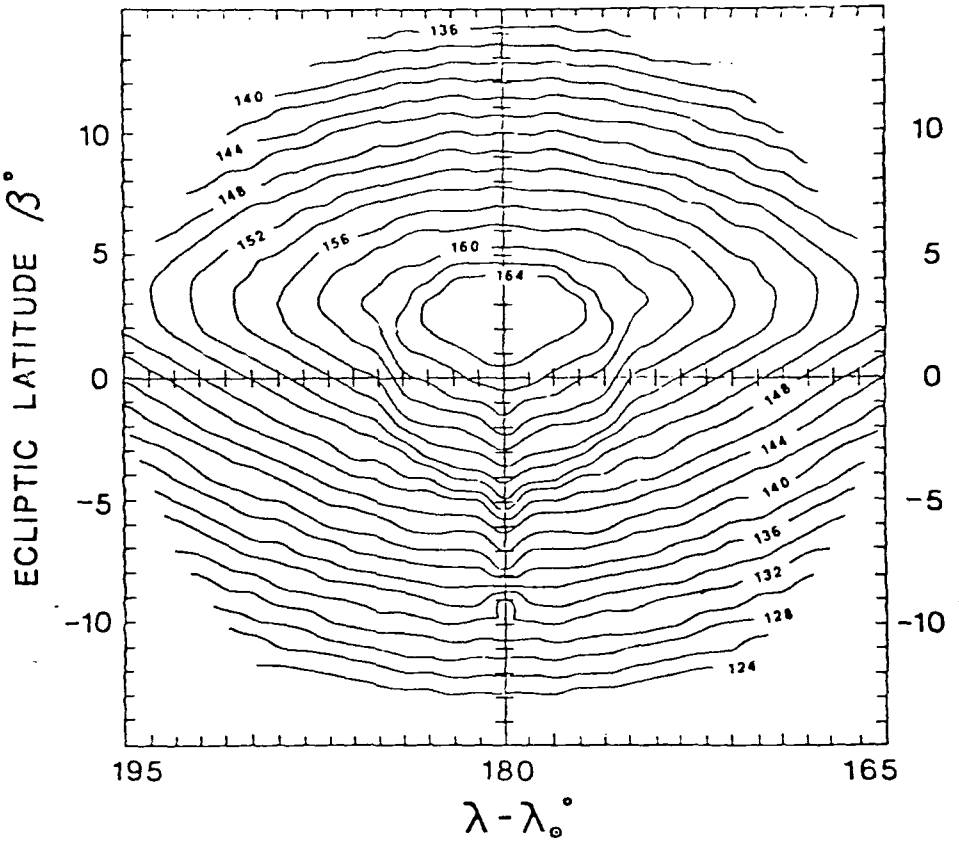
136
140
144
148
152
156
160
164
148
144
140
136
132
128
124
10
5
0
-5
-10
195
180
165
ECLIPTIC LATITUDE β°
λ - λ⊙°
DIFFERENTIAL ECLIPTIC LONGITUDE

Fig. 5

Planet. Space Sci. Vol. 28, pp. 1077-1079
© Pergamon Press Ltd., 1980. Printed in Northern Ireland

0032-0633/80/1101-1077$02.00/0

SHORT COMMUNICATION

ON THE EQUIVALENCE OF EXPRESSIONS FOR INVERTING THE 3-DIMENSIONAL ZODIACAL LIGHT BRIGHTNESS INTEGRAL

Donald W. Schuerman

Space Astronomy Laboratory
State University of New York at Albany
Executive Park East
Albany, New York 12203

(Received 9 September 1980)

Abstract - In the research notes of this journal, both Schuerman (1979, henceforth Paper I) and Buitrago (1979, henceforth Paper II) independently derived expressions for the general[1], mathematical inversion of the zodiacal light brightness integral. In this communication, it is shown that the expressions are equivalent, differing only in the choice of reference systems.

In Paper I, a system of coordinates $(r_o, h_o, \lambda'_o, \beta)$ is employed where (r_o, h_o) designates the *position* of the observer in cylindrical ecliptic coordinates and (λ'_o, β) defines the *"look" direction* in sun centered $(\lambda'_o = \lambda - \lambda_o)$ ecliptic coordinates. It was in this reference system that the 3-dimensional inversion of the zodiacal light brightness integral was first formulated (Schuerman, 1977). In Paper II, Buitrago used a different set of independent variables $(R, \beta_o, \varepsilon, i)$ to derive a result which was difficult to compare with the brief, published abstract of Schuerman (1977); Paper I was in press. In Paper II, the position of the observer is designated by (R, β_o) where R is the observer's heliocentric distance and β_o is his ecliptic latitude. The observer's "look" direction is defined by ε, the elongation angle, and i, the inclination of the scattering plane (see diagrams in Papers I and II).

In both papers it is sought to invert the brightness integral (called Z in Paper I)

$$I = \int_0^\infty \frac{P_o R_o^2}{R^2} n\sigma \, dl \, , \qquad (1)$$

[1] The only assumption being that the interplanetary dust complex is azimuthally symmetric.

where $P_o R_o^2/R^2$ is the solar flux density (ergs $cm^{-2}s^{-1}$) incident upon a dust number density n (cm^{-3}) whose average differential scattering cross section is σ ($cm^2 sr^{-1}$). The integral is over the line of sight, dl. In order to simplify the notation, we will use ψ instead of Buitrago's β_o, and we drop the subscripts and the prime on the author's independent variables: $\beta_c \to \psi$, $r_o \to r$, $h_o \to h$, $\lambda_o' \to \lambda$. If the integrand of (1) is designated by ζ, the brightness/unit line of sight, the results of both papers can be summarized as follows:

$$\left[\begin{matrix}\text{Paper I}\\ \text{eq. 23}\end{matrix}\right] \qquad \zeta(r,h,\lambda,\beta) = \frac{\partial I}{\partial r}\cos\beta\cos\lambda - \frac{\partial I}{\partial h}\sin\beta - \frac{\partial I}{r\partial\lambda}\cos\beta\sin\lambda \quad , \tag{2}$$

$$\left[\begin{matrix}\text{Paper II}\\ \text{eq. 5}\end{matrix}\right] \qquad \zeta(R,\psi,\varepsilon,i) = \frac{\partial I}{\partial R}\cos\varepsilon - \frac{\partial I}{R\partial\varepsilon}\sin\varepsilon - \frac{\partial I}{R\partial\psi}\sin\varepsilon\left(1-\frac{\cos^2 i}{\cos^2\psi}\right)^{\frac{1}{2}} \quad . \tag{3}$$

It is the purpose of this communication to point out that (2) and (3) are equivalent. The two sets of independent variables are related by

$$R^2 = r^2 + h^2 \quad , \quad \tan\psi = h/r \quad , \tag{4}$$

$$\cos\varepsilon = -\sin\psi\sin\beta + \cos\psi\cos\beta\cos\lambda \quad , \tag{5}$$

$$\cos i = \frac{\cos\psi\cos\beta\sin\lambda}{\sin\varepsilon} \quad . \tag{6}$$

Equations (4) are obvious from the coordinate definitions; (5) and (6) are derived in Paper I. The transformations of the partial derivatives in (3) are simplified by noting that for all elements along the line-of-sight, both β and i are constants; thus $\partial I/\partial\beta = \partial I/\partial i = 0$. The chain rule for the partials in (2) is then given by

$$\begin{aligned}
\frac{\partial I}{\partial r} &= \frac{\partial I}{\partial R}\frac{\partial R}{\partial r} + \frac{\partial I}{\partial\psi}\frac{\partial\psi}{\partial r} + \frac{\partial I}{\partial\varepsilon}\frac{\partial\varepsilon}{\partial r} \quad ,\\
\frac{\partial I}{\partial h} &= \frac{\partial I}{\partial R}\frac{\partial R}{\partial h} + \frac{\partial I}{\partial\psi}\frac{\partial\psi}{\partial h} + \frac{\partial I}{\partial\varepsilon}\frac{\partial\varepsilon}{\partial h} \quad ,\\
\frac{\partial I}{\partial\lambda} &= 0 + 0 + \frac{\partial I}{\partial\varepsilon}\frac{\partial\varepsilon}{\partial\lambda} \quad .
\end{aligned} \tag{7}$$

The null elements reflect the fact that $\partial R/\partial\lambda = \partial\psi/\partial\lambda = 0$; i.e., the position coordinates are independent of the "look" coordinates.

The transformation of (2) is now straightforward. As an example, we compute the coefficient of $\partial I/\partial\psi$ in (3). Substituting (7) for the partials in (2), we find the coefficients of $\partial I/\partial\psi$ combine to yield the left-hand-side (LHS) of the expression

$$\left[\begin{matrix}\text{coefficient}\\ \text{of } \partial I/\partial\psi\end{matrix}\right] \qquad \underbrace{\cos\beta\cos\lambda\frac{\partial\psi}{\partial r} - \sin\beta\frac{\partial\psi}{\partial h}}_{\text{(Paper I)}} \stackrel{?}{=} \underbrace{-\frac{\sin\varepsilon}{R}\left(1-\frac{\cos^2 i}{\cos^2\psi}\right)^{\frac{1}{2}}}_{\text{(Paper II)}} \quad . \tag{8}$$

The partials $\partial\psi/\partial r$ and $\partial\psi/\partial h$ are obtained from (4): $-\sin\psi/R$ and $\cos\psi/R$, respectively. Next, (5) is used to replace $\cos\beta\cos\lambda$ in the LHS of (8) which leaves only $\sin\beta$ as a remaining Paper I coordinate. Substituting (5) and (6) for λ in $1 = \cos^2\lambda + \sin^2\lambda$ results in a quadratic expression which can be solved for $\sin\beta$,

$$\sin\beta = -\cos\varepsilon \sin\psi \pm \cos\psi \sin\varepsilon \left(1 - \frac{\cos^2 i}{\cos^2\psi}\right)^{\frac{1}{2}} . \qquad (9)$$

The ambiguity in sign is resolved by considering the special case of $\lambda = 0$ in (5) and (6) which yields

$$\beta = \varepsilon - \psi \quad \text{for } i = 90^\circ . \qquad (10)$$

Relation (10) is preserved for the *positive* root in (9). The equivalence of (8) then trivially follows by substituting (5) and (10 with + sign) into its LHS. Alternatively, one can demonstrate the equivalence of (8) by solving the spherical triangle in Fig. 2 of Paper I.

The equivalence of the coefficients $\partial I/\partial R$ and $\partial I/\partial\varepsilon$ can be demonstrated in the same manner as that used above for $\partial I/\partial\psi$. The proof is less cumbersome than for $\partial I/\partial\psi$ and will not be given here.

As a final comment, we note that although the equivalent expressions (2) and (3) both represent the general inversion of the brightness integral, the values of all three partial derivatives cannot be obtained by a single observer moving in solar orbit. Only one (of the two) spatial derivatives can be obtained from a spacecraft. This limits the practical use of the inversion formula to "look" directions confined to a single plane, as discussed in Paper I and by Dumont *et al.* (1979), rather than the full 4π steradians.

Acknowledgements - The author wishes to thank Dr. F. Sanchez (Instituto de Astrofisica de Canarias) and Dr. J. Buitrago for helpful communications. This work was supported by the U.S. Air Force Office of Scientific Research under grant AFOSR 80-0043.

REFERENCES

Buitrago, J. (1979). *Planet. Space Sci.*, 27, 1043-1044.

Dumont, R. Papaport, M., Schuerman, D. and Levasseur-Regourd, A.C. (1979). *Space Res.* XIX, 451-454.

Schuerman, D.W. (1979). *Planet. Space Sci.*, 27, 551-556.

Schuerman, D.W. (1977). *Bull. Am. Astr. Soc.*, 9, 564-565.

BRIGHTNESS AND POLARIZATION OF THE ZODIACAL LIGHT: RESULTS OF FIXED-POSITION OBSERVATIONS FROM SKYLAB

J. L. Weinberg and R. C. Hahn
Space Astronomy Laboratory
State University of N. Y. at Albany
Albany, N. Y. 12203

ABSTRACT

In an earlier paper Sparrow *et al.* (1976) found the polarized brightness of zodiacal light to have solar color at five sky positions for which there were fixed-position observations from Skylab: north celestial pole, south ecliptic pole, vernal equinox, and two places near the north galactic pole. The brightness and degree of polarization of zodiacal light at these sky positions are derived using Pioneer 10 observations of background starlight from beyond the asteroid belt (Weinberg *et al.*, 1974; Schuerman *et al.*, 1976) and the assumption that the zodiacal light is also solar color in total light.

Ten-color observations of sky brightness and polarization were made of portions of the antisolar hemisphere from Skylab (Weinberg *et al.*, 1975; Sparrow *et al.*, 1977). Three independent quantities were determined directly from the measurements: total brightness (B_t), polarized brightness (B_p), and orientation of the plane of polarization (χ), the last more precisely referred to as azimuth of vibration. These three quantities are related to the Stokes parameters I, Q, and U, respectively.

Except in regions relatively close to the Milky Way, the observed direction and amount of polarization (χ, B_p) in these space measurements can generally be attributed entirely to zodiacal light. To isolate the zodiacal light brightness, it is necessary to remove the brightness contribution of all discrete or "resolved" stars in each 6° diameter field of view (FOV) and to subtract the background starlight (integrated starlight, diffuse galactic light, light from extragalactic sources). Thus, the zodiacal light total brightness (B_z) is obtained as the residual after a several-step subtraction process. This subtraction process has been the largest single source of error in determining the brightness of zodiacal light in observations from space and, even more so, in observations from the ground.

Skylab observations included sky-scanning and fixed-position measurements, the latter at the north celestial pole, south ecliptic pole, and vernal equinox, and at two positions near the north galactic pole. A number of sequences of filters (Table 1) were used to observe these

I. Halliday and B. A. McIntosh (eds.), Solid Particles in the Solar System, 19–22.

positions, one sequence taking 2 minutes. In the following, we briefly outline our method for evaluating discrete and, especially, background starlight at the Skylab wavelengths, so as to derive the total brightness of zodiacal light at these sky positions. The method will be developed more fully elsewhere, in conjunction with its use to isolate the zodiacal light in Skylab sky-scanning observations.

Omitting absolute calibration and the conversion of analog voltages to relative brightness and polarization, reduction of the Skylab observations involves the following major steps:

1. Determination of instrument pointing. Pointing directions are obtained by combining vehicle attitude data with telemetry data on position in the instrument's reference system and using data derived from photographs with a bore-sighted, 16mm camera. Where there are frames containing at least three or four identifiable stars, pointing is generally known to at least ±0.2°.
2. Determination of the brightness contribution of stars resolved by the instrument. A combined star catalog was generated by editing and merging data in the U.S. Naval Observatory Photoelectric Catalog (Blanco *et al.*, 1968), the Yale Catalogue of Bright Stars (Hoffleit, 1964), and the Moscow General Catalog of Variable Stars. The Skylab spectral transmittance functions were convolved with 40 stellar spectral energy distributions selected from the five luminosity classes given in Mitchell and Johnson (1969). These were used to determine the relationship of the instrument magnitude to the Johnson V magnitude as a function of the B-V color index and spectral luminosity class. This relationship was then used to convert the Johnson V magnitudes of the combined star catalog to instrument magnitudes for each Skylab filter.
3. Separation of background starlight and zodiacal light at Skylab wavelengths. The Pioneer 10/11 Imaging Photopolarimeters were used to periodically measure sky brightness and polarization in the blue (B/W 3950Å-4850Å) and red (5900Å-6900Å) at heliocentric distances beyond 1.002 AU. A two-color map of background starlight over the sky has just been completed using Pioneer 10 observations from beyond the asteroid belt (Weinberg *et al.*, 1974), where the zodiacal light was found to be negligible compared to the background starlight (Hanner *et al.*, 1974; Schuerman *et al.*, 1977). To create this map, the contributions of resolved stars (stars brighter than V magnitude = 6.5) were removed from each of 60,000 FOV's before merging data from sky-mapping observations made at six heliocentric distances between 3.27 AU and 5.15 AU. These data are used to separate background starlight and zodiacal light in those Pioneer 10/11 observations which contain both; *i.e.*, in observations at heliocentric distances less than approximately 3 AU. The Pioneer background starlight data can also be used directly in any other observations having similar spatial and discrete star resolution - and similar wavelengths (blue and red).

Table 1 illustrates our use of Pioneer red background starlight (effective wavelength 6420Å) directly with data at Skylab wavelength 6427Å. Also shown is the method used for other wavelengths in Skylab fixed-position observations at the north celestial pole.

Table 1. Observed and Derived Results at the North Celestial Pole

(1) Filter central wavelength	(2) χ	(3) B_p	(4) B_t	(5) B_{ds}	(6) B_t-B_{ds}	(7) B_{bs}	(8) B_z
4001Å	24°8	23.8	192	28.0	164	[87]	77
4748Å	27.8	18.5	154	14.3	140	63	77
5068Å	28.0	19.4	164	13.7	150	73	77
5294Å	27.7	18.3	163	12.5	151	74	77
5562Å	27.3	19.3	179	11.2	168	[91]	77
6063Å	26.7	17.9	164	11.3	153	76	77
6286Å	27.0	19.2	221	11.9	209	[132]	77
6427Å ·····	26.6···	18.7···	167···	11.6···	155·····	78····	77
7093Å	28.4	18.9	172	11.3	161	84	77
8160Å	29.4	15.4	187	11.5	176	[99]	77
Mean Values	27°4±.1	18.8±.2					77

Each value of χ, B_p, and B_t is the mean of up to 15 individual measurements.

Table 1 columns and discussion:

(2) Measured orientations of the plane of polarization; these values correspond closely to the electric vector's being perpendicular to the scattering plane.

(3) Polarized brightness (B_p), in $S_{10}(V)$ units. The $S_{10}(V)$ unit is referred to the sun; the brightnesses in this unit will have the same value at all wavelengths for radiation of solar color. Absolute calibrations at 4001Å and 8160Å appear to be high and low, respectively, as noted in a first analysis of these data by Sparrow *et al.* (1976). The mean value is determined using 8 colors only.

(4) Total observed brightnesses (B_t). These include discrete and background starlight, zodiacal light, and airglow emission; the last at 5562Å, 6286Å, and probably 8160Å.

(5) Discrete starlight (B_{ds}).

(6) Total brightness (B_t) minus discrete starlight (B_{ds}). Except for the aforementioned airglow, these differences correspond to background starlight plus zodiacal light.

(7) and (8): Background starlight (B_{bs}) and zodiacal light (B_z), respectively. For B_{bs} Skylab 6427Å is equivalent to Pioneer red, which we found (column (7)) to be 78 $S_{10}(V)$. Thus, $B_t-B_{ds}-B_{bs}=B_z=77$ $S_{10}(V)$. As seen in column (3) (see, also, Sparrow *et al.*, 1976), B_p is close to solar color. If we assume that B_z is also solar color, then $B_z=77$ $S_{10}(V)$ at all Skylab wavelengths (column (8)). B_{bs} at the other Skylab wavelengths is obtained from the corresponding differences, (6)-(8). Due to calibration difficulties and airglow emission, the bracketed values of B_{bs} are uncertain. From Pioneer blue data (effective wavelength 4360Å) we find $B_{bs}=57$ $S_{10}(V)$, in good agreement with the trend in Skylab-derived values of B_{bs}; *i.e.*, the results are consistent with the assumption of solar color for B_z.

Table 2 gives the results obtained by applying this method to all fixed-position observations. Each value of χ and B_p is a mean value obtained as shown in Table 1. Only part of the data was available for the earlier analysis of the B_p data by Sparrow *et al.* (1976), which also found

Table 2. Best Estimate of Mean Zodiacal Light - Fixed Position Observations, Skylab Mission SL-2

Target	Coordinates Equatorial α	δ	Ecliptic ε	β	Zodiacal Light χ	B_p	B_z	p
NCP	174°.2	85°.8	67°.2	65°.8	27°.4±.1	18.8±.2	77	.244
SEP	76.2	-66.6	89.8	-84.5	30.8±.3	11.4±.5	50	.228
VE	350.6	1.0	89.9	4.6	29.6±.2	25.6±.4	168	.152
NGP1	190.9	27.6	95.4	29.4	29.8±.4	17.0±.3	110	.154
NGP2	189.8	27.4	92.4	28.8	29.5±.2	17.2±.2	112	.154

B_p to be solar color. Availability of all of the data for our analysis and our use of a different solar-based $S_{10}(V)$ unit account for the slightly lower values of B_p found here. In this paper and in our studies of Pioneer 10/11 data, we follow the $S_{10}(V)$ recommendations of Sparrow and Weinberg (1976). The degree of polarization, p, is derived, not measured. It is obtained from B_p/B_z. The measured and assumed solar colors for B_p and B_z, respectively, mandate that p be grey or independent of wavelength. The p data reconfirm our earlier result (Weinberg and Hahn, 1976) and that of Dumont and Sanchez (1976) that p is greater off the ecliptic than on the ecliptic at these elongations. As noted earlier, this methodology is also being used in the reduction of the Skylab scanning data.

We thank Dr. Frank Giovane for developing the Skylab star subtraction methodology and Susan Darbyshire for assisting in the reduction of these data. This work is supported by NASA grant NSG 8040.

REFERENCES

Blanco, V.M., Demers, S., Douglass, G.G., and Fitzgerald, M.P.: 1968, *Photoelectric Catalogue, Ser. 3, Vol. 21*, U.S. Naval Obs., Washington.

Dumont, R. and Sánchez, F.: 1976, *Astron. Astrophys. 51*, pp. 393-399.

Hanner, M.S., Weinberg, J.L., DeShields II, L.M., Green, B.A., and Toller, G.N.: 1974, *J. Geophys. Res. 79*, pp. 3671-3675.

Hoffleit, D.: 1964, *Yale Catalogue of Bright Stars*, Yale University.

Mitchell, R.I. and Johnson, H.L.: 1969, *Comm. Lunar and Planetary Lab. No. 32*, University of Arizona.

Schuerman, D.W., Toller, G.N., Beeson, D.E., Tanabe, H., and Weinberg, J.L.: 1976, *Bull. Am. Astron. Soc. 8*, 503.

Schuerman, D.W., Weinberg, J.L., and Beeson, D.E.: 1977, *Bull. Am. Astron. Soc. 9*, 313.

Sparrow, J.G. and Weinberg, J.L.: 1976, in H. Elsässer and H. Fechtig (eds), *Lecture Notes in Physics, 48*, Springer-Verlag, Heidelberg, pp. 41-44.

Sparrow, J.G., Weinberg, J.L., and Hahn, R.C.: 1976, *loc cit*, pp. 45-51.

Sparrow, J.G., Weinberg, J.L. and Hahn, R.C.: 1977, *Appl. Opt. 16*, 978-982.

Weinberg, J.L. and Hahn, R.C.: 1976, in M.I. Kent, E. Stuhlinger, and S. Wu (eds), *Progress in Astronautics and Aeronautics, 48*, AIAA, New York, pp. 223-235.

Weinberg, J.L., Hanner, M.S., Beeson, D.E., DeShields II, L.M., and Green, B.A.: 1974, *J. Geophys. Res. 79*, pp. 3665-3670.

Weinberg, J.L., Sparrow, J.G., and Hahn, R.C.: 1975, *Space Sci. Instr. 1*, pp. 407-418.

THE EFFECT OF RADIATION PRESSURE ON THE RESTRICTED THREE-BODY PROBLEM

Donald W. Schuerman
Space Astronomy Laboratory
State University of N. Y. at Albany
Albany, N. Y. 12203

ABSTRACT

The classical restricted three-body problem is generalized to include the force of radiation pressure and the Poynting-Robertson effect. The positions of the Lagrangian points L_4 and L_5 are found as functions of β, the ratio of radiational to gravitational forces. The Poynting-Robertson effect renders the L_4 and L_5 points unstable on a time scale (T) long compared to the period of rotation of the two massive bodies. For the solar system, T is given by $T = [(1-\beta)^{2/3}/\beta]\ 544\ a^2$ yr where a is the separation between the Sun and the planet in AU. Implications for space colonization and a mechanism for producing asymmetries in the interplanetary dust complex are discussed; testing the latter may be possible from the Zodiacal Light/Background Starlight Experiment aboard the International Solar Polar Mission spacecraft to be launched in 1983.

A steady state solution of the motion of a β particle (a particle whose surface to volume is such that the force of radiation pressure is non-negligible) in the gravitational field of two larger, orbiting bodies of masses M_1 and M_2 is sought. It is assumed that M_1 and M_2 are in circular orbits about their common center of mass, that their angular frequency (Ω) is given by $\Omega^2 = G(M_1 + M_2)/a^3$, and that the β particle remains in the plane in which M_1 and M_2 revolve. In the rotating reference frame whose origin is the center of mass and whose angular frequency is Ω, the two components of the equation of motion of a β particle with coordinates (X,Y) are

$$\frac{\ddot{X}}{\Omega^2} - \frac{2\dot{Y}}{\Omega} = X - \frac{(1-\beta_1)\mu(X+\mu-1)}{r_1^3} - \frac{(1-\beta_2)(1-\mu)(X+\mu)}{r_2^3} \qquad (1)$$

$$\frac{\ddot{Y}}{\Omega^2} + \frac{2\dot{X}}{\Omega} = \left(1 - \frac{(1-\beta_1)\mu}{r_1^3} - \frac{(1-\beta_2)(1-\mu)}{r_2^3}\right) Y \quad . \qquad (2)$$

I. Halliday and B. A. McIntosh (eds.), Solid Particles in the Solar System, 285–288.

M_1 is located at X = 1-μ, M_2 is located at X = -μ and μ = $M_1/(M_1+M_2)$. The distances from the point (X,Y) to the centers of mass M_1 and M_2 are $r_1 = \{(x+\mu-1)^2 + Y^2\}^{1/2}$ and $r_2 = \{(x+\mu)^2 + Y^2\}^{1/2}$ respectively. The two terms on the left-hand side of equations (1) and (2) represent the acceleration and the coriolis force experienced by the β particle; the centrifugal acceleration has been placed on the right-hand side (RHS). The last two terms on the RHS's of equations (1) and (2) represent the components of the "effective" gravitational forces. These terms differ from those of the classical problem in that *each component has been reduced by a factor of the form* 1-β.

The equilibrium points L_4 and L_5 are found by setting the RHS's of equations (1) and (2) equal to zero with Y ≠ 0. The solution is

$$r_1 = (1-\beta_1)^{1/3} \equiv \delta_1 \quad , \quad r_2 = (1-\beta_2)^{1/3} \equiv \delta_2 \quad . \tag{3}$$

From solution (3) it follows that the L_4 and L_5 points exist only if all of the following conditions are satisfied: $\delta_1+\delta_2 \geq 1$, $0 < \delta_1 \leq 1$, and $0 < \delta_2 \leq 1$. These results are plotted in Fig. 1 which shows the positions of the L_4 and L_5 points as a function of β_1 and β_2 (and equivalently, δ_1 and δ_2). For application to the solar system, β_2 vanishes and δ_2 is unity; the locus of these solutions, parameterized by β_1, is the heavy arc shown in Fig. 1. (Henceforth, the subscripts on β_1 and δ_1 will be omitted). Furthermore, these solutions, when applied to the solar system (μ=1) are *stable* in the sense that a small displacement of the β particle from equilibrium will result in oscillations whose amplitude *does not* increase with time.

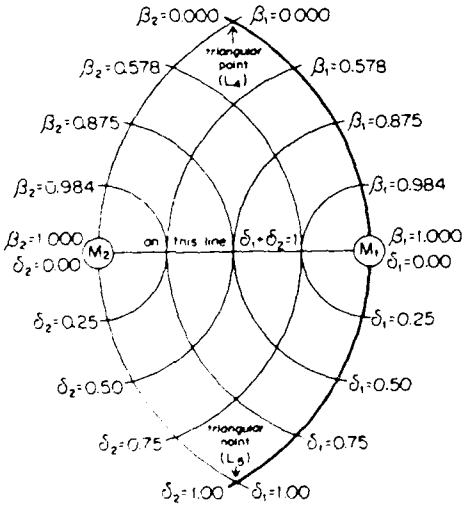

FIG. 1. The possible positions of the equilibrium points. The heavy line applies to systems with only *one* luminous body, M_1.

The results mentioned thus far have an interesting application for artificial satellites and future space colonization. It has been suggested (*e.g.*, O'Neill, 1974) that the classical triangular points of the Sun-Jupiter or Sun-Earth system would be a convenient site to locate future space colonies. Present day technology permits the construction of spacecraft whose value of β can be made or varied in the range 0<β<1. A space colony with a solar facing adjustable "sail" could thus "park" (*i.e.*, remain stationary with respect to the Sun and a planet without expending large amounts of energy) not only at the classical triangular positions but at *any* heliocentric distance out to that of the planet.

When terms representing the Poynting-Robertson effect,

$$P_x = \frac{-\beta u a\Omega}{c r_1^2}\left[\frac{\dot{X}}{\Omega} - Y + \frac{(X+\mu-1)}{r_1^2}\left(\frac{\dot{X}}{\Omega}(X+\mu-1) + \frac{\dot{Y}}{\Omega}Y\right)\right] \tag{4}$$

$$P_y = \frac{-\beta u a\Omega}{c r_1^2}\left[\frac{\dot{Y}}{\Omega} + X+\mu-1 + \frac{Y}{r_1^2}\left(\frac{\dot{X}}{\Omega}(X+\mu-1) + \frac{\dot{Y}}{\Omega}Y\right)\right] \quad , \tag{5}$$

are included on the RHS's of equations (1) and (2), the problem can still be solved analytically (to first order terms in $a\Omega/c$) in the same manner as before. The locations of the equilibrium points differ in this treatment only by small corrections of the order of $a\Omega/c$. However, *all solutions are unstable* when the Poynting-Robertson effect is taken into account. The time scale of this instability, when applied to the solar system, is given by

$$T \approx \frac{(1-\beta)^{2/3} c a^2}{3\beta M_o G} = \frac{(1-\beta)^{2/3}}{\beta} 544\ a^2\ \text{yr} \quad (a \text{ in AU's}). \tag{6}$$

A convenient and representative value for β of 0.57 makes $(1-\beta)^{2/3}/\beta = 1$. Thus, for example, the Sun-Jupiter system (a = 5.2 AU) results in $T \approx 14{,}000$ yr. This means that if a particle with $\beta = 0.57$ is displaced slightly from its equilibrium position, it will oscillate about that position and the amplitude of that motion will increase by a factor of e in 14,000 yr. (A more complete derivation of these results is given by Schuerman, 1980).

It is not at all evident that the above mechanism could lead to a significant increase in the density of interplanetary β particles along the arc schematically shown as a heavy line in Fig. 1. Other forces act on these β particles which cannot be treated by the analytical methods employed here. Interactions with the gravitational fields of intervening planets would leave large gaps in the arc of β particles. Jupiter, because of its great mass, would be particularly effective in disrupting the dust in arcs associated with other planets; conversely, dust in the Sun-Jupiter arc would be the least affected by planetary encounters. The Lorentz force due to the solar magnetic field also acts on (charged) β particles. This conservative force is roughly 40% that of the solar gravitation (Greenberg and Schuerman, 1978). The uncertainties in the charges of the β particles and in the long term fluctuations and reversals of the solar magnetic field at distances greater than 1 AU make the inclusion of the Lorentz force in this problem particularly difficult. Finally, the ions in the solar wind impinging on the β particles and the Coulomb interaction between solar wind electrons and the β particles contribute non-conservative drag forces which together are estimated to be about 30% of the Poynting-Robertson effect (Bandermann, 1967; Misconi, 1976a). These forces must surely operate to shorten the time scale (T) in equation (6).

Even if planetary encounters do not disrupt the entire arc, and even if the large but conservative Lorentz force averages out to a small effect over many solar cycles, there still remains the need for a replenishment

mechanism if an increase in the density of β particles along a planetary arc is to be expected on a "steady state" basis. The major source of replenishment for the interplanetary dust complex is thought to be cometary debris (Whipple, 1955 and 1967; Dohnanyi, 1970, 1972, and 1973). Comets shed both β particles (some with $\beta<1$) and larger ($\gtrsim 1$ μm) particles; light scattering by the latter is the main contribution to the zodiacal light. These larger particles ultimately fragment through self-collisions (Zook, 1975) or possibly by rotational bursting (Paddack and Rhee, 1975; Misconi, 1976b). It is not evident whether or not these sources of β particles provide a wide enough distribution in real space and velocity space so as to deposit a significant fraction of "zero-velocity" β particles at their appropriate equilibrium positions in times short compared to T in equation (6).

Fortunately, measurements made during the International Solar Polar Mission may determine whether or not this mechanism produces any "dust arcs" in the solar dust complex. A zodiacal light photopolarimeter (jointly designed by teams at the Ruhr-University, Bochum, FRG and the State University of New York at Albany) will map the brightness and polarization of the zodiacal light throughout the four and one-half year mission to Jupiter and back over the poles of the Sun. During the two periods of solar polar passage, the spacecraft will be in the center of the solar system but at 1.7 AU above (and below) the ecliptic plane. From these vantage points, isophotes of the zodiacal light may reveal any enhancements in the spatial density of the dust along arcs associated with planets.

This work was supported by the Air Force Office of Scientific Research (Contract F49620-78-C-0013) and by the National Aeronautics and Space Administration (JPL Contract 955137).

REFERENCES

Bandermann, L.W.: 1967, thesis, University of Maryland.
Dohnanyi, J.S.: 1970, *J. Geophys. Res.*, *75*, 3648.
Dohnanyi, J.S.: 1972, *Icarus*, *17*, 1.
Dohnanyi, J.S.: 1973, in *Evolutionary and Physical Properties of Meteoroids*, ed. C.L. Hemenway, P.M. Millman and A.F. Cook (NASA, Wash. D.C.: NASA SP 319), 363.
Greenberg, J.M., and Schuerman, D.W.: 1978, *Nature*, *275*, 39.
Misconi, N.Y.: 1976a, *Astron. and Astrophys.*, *51*, 357.
Misconi, N.Y.: 1976b, *Geophys. Res. Letters*, *3*, 585.
O'Neill, G.K.: 1974, *Physics Today*, *27*, 32.
Paddack, S.J., and Rhee, J.W.: 1975, *Geophys. Res. Letters*, *2*, 365.
Schuerman, D.W.: 1980, submitted for publication in *Ap. J.*
Whipple, F.L.: 1955, *Ap. J.*, *121*, 750.
Whipple, F.L.: 1967, in *The Zodiacal Light and the Interplanetary Medium*, ed. J.L. Weinberg (NASA, Wash. D.C.: NASA SP 150), 409.
Zook, H.A.: 1975, *Planet. Space Sci.*, *23*, 1391.

EVIDENCE THAT THE PROPERTIES OF INTERPLANETARY DUST BEYOND 1 AU ARE NOT HOMOGENEOUS

Donald W. Schuerman
Space Astronomy Laboratory
State University of N. Y. at Albany
Albany, N. Y. 12203

ABSTRACT

Traditionally, earth-based observations of the zodiacal light (ZL) require two assumptions for further analysis: (A1) the dust density (n) is a power of heliocentric distance (R), $n \propto R^{-\nu}$; (A2) the nature (scattering cross section, σ) of the dust is independent of location, $\sigma(r,h,\theta)=\sigma(\theta)$. Observations from Pioneer 10 do *not* verify these assumptions.

Both two-dimensional inversion techniques (Schuerman, 1979a) and more traditional methods of analysis (Hanner *et al.*, 1976) have been performed on portions of the ZL observations made from Pioneer 10/11 spacecraft. In developing the three-dimensional form of the ZL inversion (Schuerman, 1979b; henceforth called Paper I), it was realized that this more general technique should be applied to the Pioneer data because the velocity vectors of the spacecraft were not confined to the ecliptic plane. The previously mentioned analyses examined data with viewing directions parallel to the ecliptic; the three-dimensional inversion requires viewing along a great circle (see Fig. 1) containing (1) the line ($\mathbf{n}$) which is both normal to the observer-Sun line and parallel to the ecliptic and (2) the spacecraft velocity vector ($\mathbf{s}$). This great circle is called the inversion plane in Paper I where its geometric construction and the notation used here are defined in more detail. The angle ϕ is the inclination of the inversion plane to the ecliptic, and viewing in the direction of $\mathbf{n}$

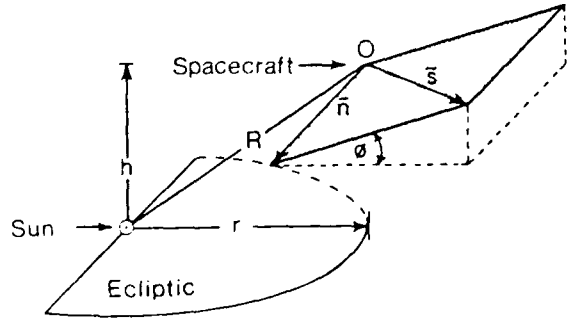

Fig. 1. Definition of the inversion (shaded) plane; it is normal to the r,h plane and contains $\mathbf{s}$, the direction of motion of the spacecraft.

I. Halliday and B. A. McIntosh (eds.), Solid Particles in the Solar System, 71–74.

Table 1

COORDINATES OF SPACECRAFT POSITION (r,h in AU) AND VALUES OF THE INCLINATION OF THE INVERSION PLANE (ϕ in deg) AS A FUNCTION OF HELIOCENTRIC DISTANCE (R in AU)

R:	1.010	1.150	1.171	1.349	1.453	1.652	1.865	2.294	2.413	2.467	2.641	2.938
r:	1.010	1.150	1.171	1.349	1.452	1.651	1.864	2.292	2.412	2.465	2.640	2.937
h:	-.009	-.030	-.032	-.045	-.051	-.060	-.067	-.079	-.081	-.082	-.085	-.089
ϕ:	-12.9	-8.60	-8.04	-4.11	-3.29	-2.60	-2.10	-1.19	-1.05	-1.01	-0.82	-0.51

corresponds to an elongation of $\varepsilon = 90°$. The observer (spacecraft) is located by cylindrical ecliptic coordinates (r,h). Table 1 lists the values of ϕ and h as a function of R($\simeq$r) for Pioneer 10. Notice that ϕ is small as is the ratio h/r. Nevertheless, we have isolated those Pioneer data having views along the inversion plane and have analyzed those data via both inversion and traditional methods. The former analysis will be published elsewhere. The blue channel brightness data in units of $S_{10}(V)$ are shown in Figure 2. The total ZL brightness (Z) as a function of ε was derived for 12 distinct heliocentric distances in order to generate this $Z(R,\varepsilon)$ surface. The values of Z have been smoothed somewhat by a curve-fitting procedure which also yields a measure of the statistical uncertainty (σ_Z) in Z at each point on the surface. Now we can apply the traditional method of ZL analysis: for each value of ε, we fit a power law of the form $Z \propto R^{\alpha}$ where $\alpha = -(1+\nu)$; see, for example, Leinert, (1975). *If assumptions* A1 *and* A2 *are correct, a single value of* α *should apply to all values of elongation.*

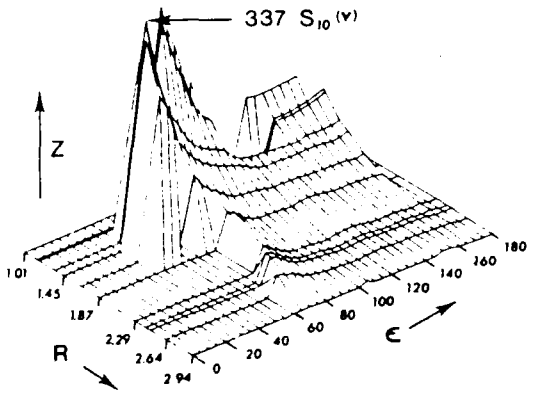

Fig. 2. The brightness (Z) of the ZL as a function of heliocentric distance (R) and elongation (ε). Viewing directions are confined to the inversion plane.

The logZ vs logR plot in Figure 3 shows a typical example of the fitting procedure used to determine α, the slope of the assumed straight line, for $\varepsilon = 115°$. Each data point on the fit is represented by two numbers of the form Z/σ_Z. The vertical error bars represent the corresponding uncertainty in logZ; $\sigma_{\log Z} = \ln(10)\ \sigma_Z/Z$. Notice that even though some data points have remarkably well determined (statistically speaking) values (3/2, 4/1, etc...), the innate mathematical properties of the assumed $Z \propto r^{\alpha}$ relation produce large uncertainties in logZ when Z is small. (Also, Z itself becomes more difficult to separate from the background starlight for

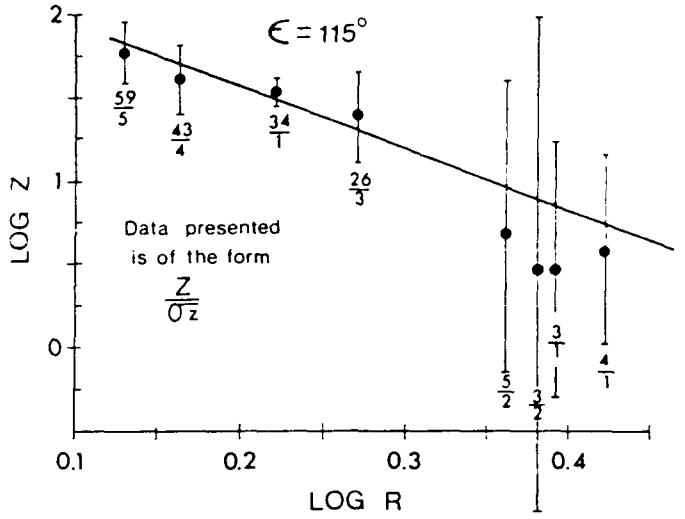

Fig. 3. LogZ vs LogR for $\epsilon = 115°$. The slope of the fitted line is $\alpha = -(1+\nu)$. The number pairs represent the data in the form Z/σ_z. The vertical bars are the uncertainty in logZ given by $\ln(10)\ \sigma_z/Z$.

observations made at large ε and R. In this regard, ZL studies made from outgoing spaceprobes require very *different* data handling techniques than those used for solar approaching probes like Helios.) Following standard statistical practice, we have weighted each data point by $(\sigma_{\log Z})^{-2}$ in determining the slope α. For the example shown in Figure 3, $\alpha = -3.6 \pm 1.4$.

Fitted values of α were obtained in the above manner for all $70° < \epsilon < 175°$ in intervals of $\Delta\epsilon = 5°$. Figure 4 depicts the result of those fits as a function of ε. The vertical bars indicate the uncertainty in α. Earlier and independent Pioneer results by Hanner *et al.* (1976) are shown as the shaded rectangle. Their estimates of α are in agreement with those found here over the limited range of elongation that they considered. However, we find a *systematic decrease in* α *for* $85° \lesssim \epsilon \lesssim 125°$. It is significant that near $\epsilon = 90°$ the "dip" in α can not be attributed to viewing in the inversion plane; the line of sight is exactly parallel to the ecliptic for $\epsilon = 90°$. Yet, it is near this direction that our results differ most from the $\alpha = -2.3$ value reported from Helios (Link *et al.*, 1976). As a final check on our results, we similarly analyzed the in-ecliptic Pioneer data previously published by Schuerman (1979a). The paucity of that data restricts the analysis to $\epsilon > 110°$. Nevertheless, the same general trend was found as denoted by the x's in Figure 4. The systematic drop of α towards $\epsilon = 100°$ is evident, and the scatter in those results is well contained within the envelope of our error bars.

Although we are pursuing other explanations, some of which address the fact that h/R is not exactly zero, we tentatively maintain that

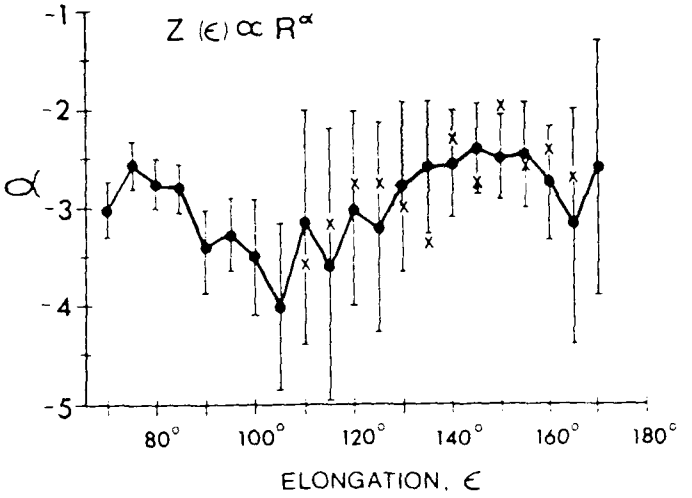

Fig. 4. Values of the index α (in $Z \propto R^{\alpha}$) as a function of elongation (ε). The circles and associated error bars refer to the data shown in Fig. 2. Data points marked by x's refer to *in-ecliptic* Pioneer data previously presented by Schuerman (1979a). The shaded rectangle approximates the earlier and independent Pioneer results of Hanner *et al.* (1976). If the scattering properties of the dust are independent of position, α should have the same value for all ε.

observational evidence now exists that either assumption A1 or A2 or both are incorrect. In fact, assumption A2 has no theoretical support whatsoever. On the contrary, most forces tend to separate the dust particles (as a function of R) according to their charge to mass ratios, surface area to volume, etc. If the results presented here are verified, it means that optical observations from space can truly begin to address the dynamics governing the solar system dust complex.

This work was supported by the Air Force Office of Scientific Research under contract F49620-78-C-0013.

REFERENCES

Hanner, M.S., Sparrow, J.G., Weinberg, J.L., and Beeson, D.E.: 1976, in *Lecture Notes in Physics 48*, ed. H. Elsasser and H. Fechtig (Heidelberg: Springer-Verlag), 29.
Leinert, C.: 1975, *Space Sci. Rev.* 18, 281.
Link, H., Leinert, C., Pitz, E., and Salm, N.: 1976, in *Lecture Notes in Physics 48*, ed. H. Elsasser and H. Fechtig (Heidelberg: Springer-Verlag), 24.
Schuerman, D.W.: 1979a, *Space Res. XIX*, 447,
Schuerman, D.W.: 1979b, *Planet. Space Sci.*, 27, 551.

THE SYMMETRY PLANE OF THE ZODIACAL CLOUD NEAR 1 AU

Nebil Y. Misconi
Space Astronomy Laboratory
State University of N. Y. at Albany
Albany, N. Y. 12203

ABSTRACT

Analysis of zodiacal light observations from Mt. Haleakala, Hawaii show that the symmetry plane of the zodiacal cloud near 1 A.U. is close to the invariable plane of the solar system. Since the symmetry plane of the inner zodiacal cloud is close to the orbital plane of Venus (Misconi and Weinberg, 1978; Leinert *et al.*, 1979), we suggest that the symmetry plane changes inclination with heliocentric distance.

INTRODUCTION

The location in space of the plane of maximum dust density (symmetry plane) of the zodiacal cloud has important implications for the dynamics of solid particles in the solar system. These implications are related to questions such as the gravitational perturbations of the planets on the dust, the effects of solar magnetic forces, and the general dynamical history of dust ejected from comets. Helios 1 and 2 zodiacal light measurements near the region of 1 A.U. (Leinert *et al.*, 1979) find that the symmetry plane in this region has an inclination $i = 3 \pm 0.3°$ and ascending node $\Omega = 87 \pm 4°$, which is different from that of the invariable plane of the solar system ($i = 1.6°$, $\Omega = 107°$). At the same time, ground-based observations at Tenerife in the Canary Islands (Dumont and Sanchez, 1968) and satellite observations from the satellite D2A (Dumont and Levasseur-Regourd, 1978) find the symmetry plane close to the invariable plane near 1 A.U.

In the present study an attempt is made to obtain additional data on the location of the symmetry plane near the Earth's orbit using ground-based observations of the zodiacal light from Mt. Haleakala, Hawaii taken by Weinberg and Mann (1967).

THE OBSERVATIONS

Two nights of observations were found to be suitable for this purpose: the evenings of 23 and 24 February, 1968. These photoelectric

I. Halliday and B. A. McIntosh (eds.), Solid Particles in the Solar System, 49–53.

observations were taken using a narrow band filter centered at 5300 Å (Weinberg and Mann, 1967). The photometer made almucantar scans of the evening zodiacal light cone in 5° steps of elevation from 10 to 45°.

Fig. 1 shows an isophote map of the zodiacal light brightness in ecliptic coordinates $(\lambda-\lambda_\odot,\beta)$ on February 24, 1968. Details of the data reduction and the method of finding the photometric axis (dashed line) were given earlier (Weinberg, 1964; Misconi, 1976 and 1978). The displacement in ecliptic latitude of the photometric axis is found to be between 1 and 1.25° from the ecliptic plane. In Fig. 2, we show the displacements from the ecliptic plane of the observed plane (dashed line) of maximum brightness on two nights in February, 1968, at elongation angles 50-90° from the Sun. The predicted displacements of the invariable plane and the orbital plane of Venus, and the extension of the symmetry plane found by Misconi and Weinberg (1978) correspond to what would be observed if the dust that contributes most to the maximum brightness were in these planes (Misconi, 1977). It is clear that the observed "plane" departs from the symmetry plane of the inner zodiacal cloud and approaches the invariable plane near the Earth's orbit: we find that the inclination decreases from $i \approx 2.7°$ at $\varepsilon \approx 50°$ to $i \approx 1.8$ to 2° at $\varepsilon \approx 90°$.

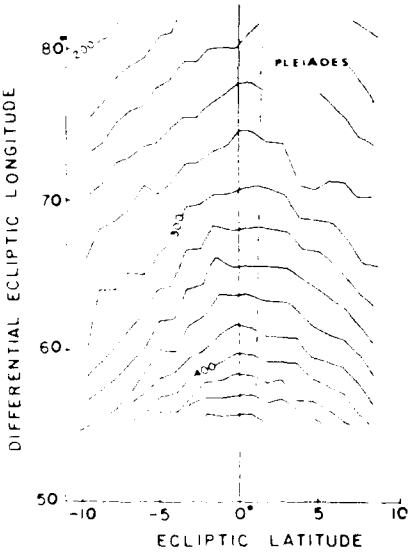

Fig. 1. Brightness contours for the evening zodiacal light on February 24, 1968 in ecliptic coordinates $(\lambda-\lambda_\odot,\beta)$.

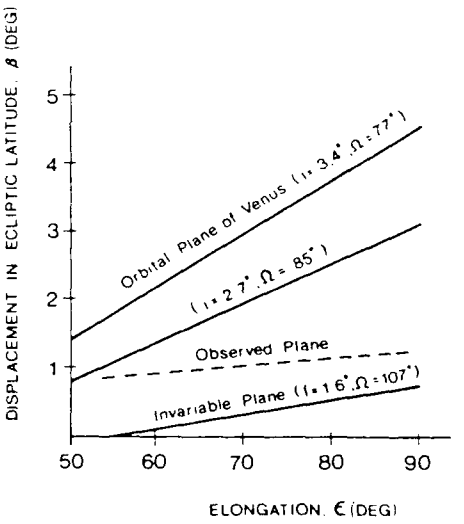

Fig. 2. Predicted displacements in ecliptic latitude (solid lines) of the orbital plane of Venus, extension of the symmetry plane of the inner zodiacal light (ε 32-50°) found by Misconi and Weinberg (1978), and the invariable plane, as a function of elongation angle. The observed symmetry plane in this region is shown by the dashed line.

At the same time, Leinert *et al.* (1979) found that a single inclination, $i = 3 \pm 0.3°$, applies over this entire range of elongation. As noted earlier, Dumont and Sanchez (1968) and Dumont and Levasseur-Regourd (1978) find the symmetry plane near 1 A.U. to be close to the invariable plane. Fig. 3 sketches the relative positions of the observed symmetry plane (dashed line) by Leinert *et al.* (1979), our observed symmetry "surface" as we prefer to call it (solid line), the invariable plane, the orbital plane of Venus, and the solar equatorial plane.

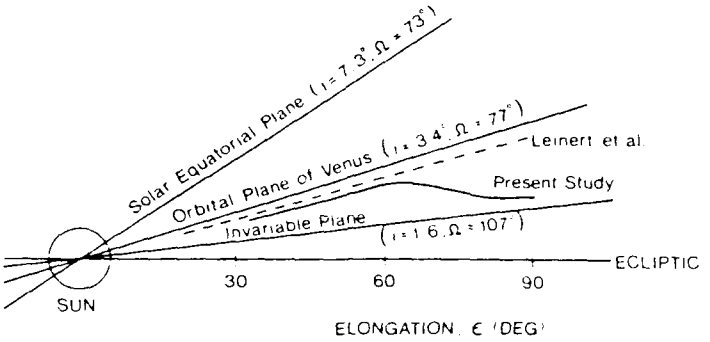

Fig. 3. A sketch of the relative inclinations from the ecliptic plane as a function of elongation: for the solar equatorial plane, the orbital plane of Venus and the invariable plane. Also shown is the position of the symmetry plane found by Leinert *et al.* (dashed line) and our combined results over this range of elongation.

DISCUSSION OF RESULTS

It is found that the symmetry plane of the zodiacal cloud at elongation angles 50-90° does not continue to be close to the orbital plane of Venus but rather departs from it and approaches the invariable plane. In view of this result one must re-evaluate the dynamical forces influencing the spatial distribution of the dust. If one considers the effects of the solar magnetic forces found by Grün and Morfill and reported in this symposium it would seem that the zodiacal cloud should have one symmetry plane decreasing smoothly in inclination with increasing heliocentric distance. Our result shows this tendency, but additional data are needed. Since the inclination of the inner part of the observed plane is 2.7° and the inclination of the solar equatorial plane is 7.3°, the solar magnetic forces have not yet achieved a symmetry to the solar equatorial plane. This fact raises questions about the lifetime of these effects and the origin of the dust in the inner region of the solar system.

It is not possible on an observational basis alone to distinguish between the gravitational effects of Venus and solar electromagnetic forces on the dust. This comes about from the fact that the solar equatorial plane and the orbital plane of Venus have almost the same ascending nodes ($\Omega = 73°$ and $\Omega = 77°$, respectively). Therefore, the question

of what is influencing the dust distribution is still unanswered. A dynamical evaluation of the gravitational influence of the inner planets on the dust distribution is needed before one can discriminate between these effects.

New observations of the zodiacal light are scheduled from Mt. Haleakala at ε = 50-180° to provide more information on the symmetry plane in these regions.

We thank D. Beeson and Tani Engel for assistance. Supported by NASA grant NSG 7093 and by Air Force Office of Scientific Research Contract F 49620-78-C-0013.

REFERENCES

Dumont, R., Sanchez, F.: 1968, *Ann. Astrophys.* 31, 293.
Dumont, R., Levasseur-Regourd, A.C.: 1978, *Astron. and Astrophys.* 64, 9.
Leinert, C., Hanner, M., Richter, I., Pitz, E.: 1979, *Astron. and Astrophys.*, in Press.
Misconi, N.Y.: 1976, *Astron. and Astrophys.*, 51, 357.
Misconi, N.Y.: 1977, *Astron. and Astrophys.*, 61, 497.
Misconi, N.Y., Weinberg, J.L.: 1978, *Science* 200, 1484.
Weinberg, J.L.: 1964, *Ann. Astrophys.*, 27, 718.
Weinberg, J.L., Mann, H.M.: 1967, in *Proc. Symposium on the Zodiacal Light and the Interplanetary Medium*, NASA SP-150, ed. J.L. Weinberg, 3.

DISCUSSION

Grün: Electromagnetic effects (Grün and Morfill, this volume) perfectly account for your observed variation of the zodiacal light symmetry plane with solar distance, i.e., the increase of inclination toward the Sun. In particular, the observed longitude of the ascending node outside the Earth's orbit supports the importance of the solar equator and contradicts the gravitational influence of Venus on dust particles outside the Earth's orbit.

Misconi: Electromagnetic effects are certainly one source affecting the symmetry plane of the zodiacal cloud. From these effects one would expect a smooth decrease in the inclination of the symmetry plane away from the Sun, whereas our observations show an irregular decrease in inclination. We agree that the fact that the symmetry plane is near the orbital plane of Venus does not necessarily mean that the dust is perturbed gravitationally by Venus. But, unless the lack of a gravitational effect by Venus is shown through a treatment using perturbation techniques - which to our knowledge has not been done - gravitational effects along with electromagnetic effects should continue to be considered as potential forces affecting the symmetry plane. Our observations find the symmetry plane near the orbital plane of Venus only at heliocentric distances between 0.5 and 0.8 AU, not outside the Earth's orbit.

Roach: How does Dr. Tanabe's measurement of the inclination near the Gegenschein compare with measurements out to Earth?
Misconi: Dr. Tanabe's results show that the symmetry plane outside the Earth's orbit decreases in inclination to a value of 0.5° and an ascending node close to that of the orbital plane of Venus; i.e., a general decrease in the inclination away from the Sun. Dr. Tanabe also suggests that the combined masses of the Earth and Venus are affecting dust outside the Earth's orbit.

Burns: A calculation has recently been completed (Burns, J.A., Hamill, P., Cuzzi, J.N. and Durisen, R.: 1979, Astron. J. in press) that might pertain to the question of gravitational perturbation of the symmetry plane. We studied analytically the out-of-plane perturbations of a particle in Saturns's ring as affected by an inclined satellite of Saturn and the planet's oblateness. We found that the ring particles suffered short - period oscillations of amplitude $(m_{part}/M)(a/a_{part})^3$ $a(\sin i_{part})$ as the particle passed under the perturbing satellite. The long - period perturbations were smaller than this but of the same form, and amounted to a smooth precession about the Laplace plane which lies between the perturber's orbital plane and the planet's equatorial plane. The Laplace plane moved closer and closer to the perturber's plane as the particle was further away from the planet; the plane was warped. Many satellite perturbers were not studied but I would expect that the plane of symmetry of Saturn's ring would be due to the global perturbation of all satellites with only small local effects due to individual satellites.
Misconi: It would be interesting to see similar calculations done for Venus.

Cook: The exchange which we have just heard appears to neglect the averaging effect of integrating along the line-of-sight. If we start with symmetry about the solar equator close to the Sun and end with the Gegenschein necessarily being close to the ecliptic at the other end, we must have local latitudes of symmetry which correspond to a steady decrease of the apparent inclination of the plane of symmetry as we move away from the Sun. If, in addition, the local Laplace plane plays a role, then the pattern will show a wavy structure - an effect which is probably beyond the reach of observations.

Leinert: Plotting the predicted ecliptic latitude of the point of maximum zodiacal light brightness makes it appear as if a determination of the plane of symmetry in the F-corona was not possible. This is misleading. The problem can be avoided by plotting the inclination angle instead of ecliptic latitude. Also it might be useful to check by model calculations whether the approximation used is still good at very small and very large elongations.
Misconi: Use of the inclination angle is a better measure of the maximum brightness but not of the photometric axis in the F-corona. We believe that information on the symmetry plane can best be obtained by scanning perpendicular to the ecliptic plane and by finding the displacement of the photometric axis in ecliptic latitude. Our method of prediction is also reliable at small and large elongations.

Abstract of the Dissertation

A STUDY OF GALACTIC LIGHT, EXTRAGALACTIC LIGHT, AND GALACTIC STRUCTURE USING PIONEER 10 OBSERVATIONS OF BACKGROUND STARLIGHT

by

Gary Neil Toller

Doctor of Philosophy

in

Earth and Space Sciences
(Astronomy Program)

State University of New York at Stony Brook

1981

An observational and theoretical study of the diffuse astronomical background sky brightness (background starlight) is carried out. The brightness is determined over 95% of the sky using Pioneer 10 photometric measurements in sky regions where the zodiacal light is negligible (heliocentric distances $\geq$ 3 A.U.). Brightness levels are presented at blue (3950-4850Å) and red (5900-6800Å) wavelengths. The B-R color index distribution is established over the celestial sphere.

Pioneer 10 results are compared with previous star count and ground based photometric studies to separate background starlight

into its constituent parts: integrated starlight, diffuse galactic light (DGL), and cosmic light. Significant errors are found in published star count results at low galactic latitudes. The galactic latitude (b^{II}) and longitude (l^{II}) dependences of integrated starlight and the variation of DGL with b^{II} are determined. A value of 1.35 ± 1.3 $S_{10}(V)_{G2V}$ is deduced for the cosmic light brightness at blue wavelengths near the galactic poles. The integrated light from discrete galaxies adequately explains this component of the background starlight.

A computer model of our galaxy, incorporating detailed interstellar absorption data and consistent with the brightness distribution observed from Pioneer 10, has been constructed for the purpose of studying background starlight. The model computes the emitted and observed brightness from any volume element. Knowledge of the brightness and absorption distributions, coupled with the Henyey-Greenstein phase function, permits calculation of DGL brightnesses. The relation between DGL, direct starlight, and extinction along the line of sight is established. Possible values for the albedo and $\left\langle \cos\theta_{sca} \right\rangle$ for the interstellar dust at blue wavelengths are deduced.

A small influence of galactic spiral structure on surface brightness levels exists at $l = 2°$ (Sagittarius arm), $l = 69°$ (Orion arm), and $l = 288°$ (Carina arm). No indication of spiral structure effects in the directions of nine other brightness maxima

and minima is discerned. A correlation between brightness features and interstellar extinction is established. Analysis of the distribution of brightness peaks and dips and the location of the brightness symmetry plane establishes the sun's elevation above the galactic plane as 12.2 ± 2.1 pc.

Calculations of the Light Scattered by Randomly Oriented Ensembles of Spheroids of Size Comparable to the Wavelength

by

Richard W. Schaefer

1980

State University of New York at Albany

COLLEGE OF ARTS AND SCIENCES

The dissertation submitted by

Richard W. Schaefer

under the title

Calculations of the Light Scattered by Randomly Oriented Ensembles of Spheroids of Size Comparable to the Wavelength

has been read by the undersigned. It is hereby recommended for acceptance to the Faculty of the University in partial fulfillment of the requirements for the degree of Doctor of Philosophy.

Warren J. Wiscombe	NOVEMBER 28, 1980
Gerald A. Silverman	November 17, 1980
Keith F. Ratcliff	November 26, 1980
Edwin D. Reilly Jr.	November 26, 1980

Recommended by the Department of _____

_____, Chair.

Recommendation accepted by the Dean of Graduate Studies for the Graduate Academic Council.

_____

_____

Abstract

Asano and Yamamoto's(1975) solution of the scattering by homogeneous spheroids of size comparable to the wavelength has been checked and used to calculate selected results. The entire solution has been rederived as a check and presented in detail as a guide to further development. Test results between the computer code developped here and that of Asano's show good agreement; in addition, results from two other recently developped theoretical methods agree with the corresponding results here to within published accuracy. Comparisons are also shown to laboratory measurements; those of the Microwave Scattering Facility(State University of New York--Albany, now at the University of Florida in Gainesville) agree well for all measurements. Finally, results are shown for the scattering by a selection(cf. Table I) of randomly oriented ensembles of spheroids. All six independent elements of the Mueller matrix along with the extinction, scattering, and phase lag cross-sections and the asymmetry factor have been calculated. From the calculations here and previous results reported by other authors, the scattering by spheroids has been discussed and characterized.

Scattering by Ensembles of Small Particles

Experiment, Theory and Application

by

Bo Å. S. Gustafson

Reports from the Observatory of Lund, No. 17

1980

ISSN 0349-4217

Abstract

A hypothetical selfconsistent picture of evolution of prestellar interstellar dust through a comet phase leades to predictions about the composition of the circum-solar dust cloud. Scattering properties of thus resulting conglomerates with a "bird's-nest" type of structure are investigated using a micro-wave analogue technique. Approximate theoretical methods of general interest are developed which compare favorably with the experimental results. The principal features of scattering of visible radiation by zodiacal light particles are reasonably reproduced. A component which is suggestive of β-meteoroids is also predicted.

Key words: Light scattering by ensembles of small particles — cometary debris — interplanetary dust — zodiacal light.